Redox Biology 37 (2020) 101735

Contents lists available at ScienceDirect

Redox Biology

journal homepage: www.elsevier.com/locate/redox

Research Paper

ADAM17 cytoplasmic domain modulates Thioredoxin-1 conformation and activity

Rute A.P. e Costa [a,2], Daniela C. Granato [a,2], Luciana D. Trino [a], Sami Yokoo [a], Carolina M. Carnielli [a], Rebeca Kawahara [a,1], Romênia R. Domingues [a], Bianca Alves Pauletti [a], Leandro Xavier Neves [a], Aline G. Santana [a], Joao A. Paulo [b], Annelize Z.B. Aragão [a], Fernanda Aparecida Heleno Batista [a], Ana Carolina Migliorini Figueira [a], Francisco R. M. Laurindo [c], Denise Fernandes [c], Hinrich P. Hansen [d], Fabio Squina [e], Steven P. Gygi [b], Adriana F. Paes Leme [a,*]

[a] Laboratório Nacional de Biociências, LNBio, CNPEM, Campinas, São Paulo, Brazil
[b] Department of Cell Biology, Harvard Medical School, Boston, USA
[c] Instituto Do Coração, Faculdade de Medicina, Universidade de São Paulo, São Paulo, São Paulo, Brazil
[d] Department of Internal Medicine I, University Hospital Cologne, CECAD Research Center, Cologne, Germany
[e] Universidade de Sorocaba, Departamento de Processos Tecnológicos e Ambientais, São Paulo, Brazil

ARTICLE INFO

Keywords:
ADAM17
Thioredoxin-1
Dimerization
Mass spectrometry
iodoTMT
Redox signaling

ABSTRACT

The activity of Thioredoxin-1 (Trx-1) is adjusted by the balance of its monomeric, active and its dimeric, inactive state. The regulation of this balance is not completely understood. We have previously shown that the cytoplasmic domain of the transmembrane protein *A Di*sintegrin *A*nd *M*etalloprotease 17 (ADAM17cyto) binds to Thioredoxin-1 (Trx-1) and the destabilization of this interaction favors the dimeric state of Trx-1. Here, we investigate whether ADAM17 plays a role in the conformation and activation of Trx-1. We found that disrupting the interacting interface with Trx-1 by a site-directed mutagenesis in ADAM17 (ADAM17cyto^{F730A}) caused a decrease of Trx-1 reductive capacity and activity. Moreover, we observed that ADAM17 overexpressing cells favor the monomeric state of Trx-1 while knockdown cells do not. As a result, there is a decrease of cell oxidant levels and ADAM17 sheddase activity and an increase in the reduced cysteine-containing peptides in intracellular proteins in ADAM17cyto overexpressing cells. A mechanistic explanation that ADAM17cyto favors the monomeric, active state of Trx-1 is the formation of a disulfide bond between Cys^{824} at the C-terminal of ADAM17cyto with the Cys^{73} of Trx-1, which is involved in the dimerization site of Trx-1. In summary, we propose that ADAM17 is able to modulate Trx-1 conformation affecting its activity and intracellular redox state, bringing up a novel possibility for positive regulation of thiol isomerase activity in the cell by mammalian metalloproteinases.

1. Introduction

Trx-1 is a key component of the cellular redox system, also comprising NADPH and thioredoxin reductase (TrxR) that provides electrons to various enzymes [1]. This system maintains the redox state of the cell, in concert with other enzymatic and non-enzymatic antioxidant systems, such as superoxide dismutase (SOD1 and SOD2), and glutathione. The evolutionarily conserved metalloproteinase ADAM17, originally discovered as TNFα-converting enzyme (TACE), is the major sheddase for EGF receptor ligands and various surface proteins [2].

Both ADAM17 and Trx-1 are involved in many physiological and pathological processes in the cell. ADAM17 is particularly implicated in inflammation processes [3,4] and the protection of the central nervous system [5]. Also, inhibitors of ADAM17 and matrix metalloproteases (MMP) serve as beneficial adjuvants in bacterial meningitis therapy. Besides, the shedding of growth factors, ADAM17 is necessary for tumor

* Corresponding author.
E-mail address: adriana.paesleme@lnbio.cnpem.br (A.F. Paes Leme).
[1] Note: Department of Molecular Sciences, Macquarie University, Sydney, Australia (Present address).
[2] The authors contributed equally to this work.

https://doi.org/10.1016/j.redox.2020.101735
Received 14 July 2020; Received in revised form 26 August 2020; Accepted 17 September 2020
Available online 24 September 2020

progression and growth, and also contributes to inflammation in tumors [5,6].

Another interesting mechanism that has recently been proposed for ADAM17 concerning its role in inflammatory diseases, is the possible connection with SARS-CoV-2 effects by cytokine storm generation. It has been proposed that the possible molecular mechanism that leads to the acute respiratory distress syndrome (ARDS) in COVID-19 patients is caused by the massive release of proinflammatory cytokines, known as cytokine storm [7]. The major contributors for cytokine storm are the proinflammatory cytokines IL-6 and TNF-α [8,9]. ADAM17 also known as TACE (Tumor necrosis factor-alpha converting enzyme) can be one of the main players involved in this process. It is well known that ADAM17 affects the biology of TNF-α and IL-6 [10–13], leading to the speculation that inhibition of ADAM17 might present a positive response in autoimmune diseases [11]. With that, some studies have suggested that potential treatments for SARS-CoV-2 most destructive complications could help improve the life expectancy of the infected patients [7,8,14–16]. Taking this rationale into account, ADAM17 inhibitors, such as Trx-1, could be promising strategies for future studies to minimize the ADAM17 extracellular role in shedding and possibly cytokine storm effect observed in patients infected with SARS-CoV-2.

Furthermore, regarding the inflammation process, Trx-1 is an oxidative stress-limiting protein with anti-apoptotic properties and shows an ambiguous function in terms of inflammation. It has been shown that Trx-1 might exert atheroprotective effects by promoting macrophage differentiation into the M2 anti-inflammatory phenotype [17]. The ability of Trx-1 to promote differentiation of macrophages into an alternative, anti-inflammatory phenotype may explain its protective effects in cardiovascular diseases, suggesting a link between oxidative stress and cardiovascular diseases. However, it has also been shown that the Trx-1 pathway enables nuclear NF-κB DNA-binding and thereby pro-inflammatory responses in monocytes and dendritic cells [18]. Moreover, independent of this activity, Trx-1 is critical for NLRP3 inflammasome activation and IL-1β production in macrophages by detoxifying excessive ROS levels [19–21]. Inflammation often complicates diseases associated with oxidative stress. It has been shown that inflammatory macrophages release proteins with specific forms of cysteine oxidation to disulfides, particularly glutathionylation [18,22,23]. Redox proteomics identified peroxiredoxin 2 (PRDX2) as a protein released in the glutathionylated form by inflammation both *in vivo* and *in vitro*, and extracellular PRDX2 then triggers the production of TNF-α, one of the main substrates of ADAM17 [22]. Together, these studies indicate that redox-dependent mechanisms, in an oxidative cascade, can induce inflammation and that targeting Trx1 may be exploited to treat inflammatory diseases, in the same manner that has been suggested for ADAM17. This leads to the suggestion that by targeting the Trx-1/ADAM17 interaction it is possible to modulate the downstream inflammation scenario promoted by different diseases. However, in the past, unspecific elimination of ROS by the use of low molecular mass antioxidant compounds was not successful in counteracting disease initiation and progression in clinical trials [18].

Trx-1 is conserved among species and contains 105 amino acid residues. Of its five cysteine residues, two are part of the catalytic site (Cys^{32} and Cys^{35}) and the remaining three (Cys^{62}, Cys^{69}, and Cys^{73}) are available for physiological modification. Cys^{62} and Cys^{69} are potential sites for S-nitrosylation but can also form a disulfide bond with each other. Cys^{73} is localized on a hydrophobic patch of the protein surface and can contribute to an intermolecular disulfide bond (Trx-1 homodimer) but is also a site for glutathionylation (GS-ylation).

Homodimerization (Cys^{73}-Cys^{73}) suppresses the functionality of Trx-1, since the dimer hides the catalytic site of the enzyme, rendering it no longer available as a substrate for thioredoxin reductase [24]. The oxidation or reduction of this bridge is dependent on the redox state of the cell [25]. Thus, the Trx-1 monomer-dimer balance is important to regulate the catalytic activity of Trx-1 [26].

Previously, we described the interaction between ADAM17 and Trx-1 [27], which has a negative effect upon ADAM17 activity. This interaction is in the opposite location of the catalytic site of Trx-1. A recent work from our group [28] has shown that ADAM17/Trx-1-interacting interface was destabilized by a mutation in Trx-1 ($Trx\text{-}1^{K72A}$), favoring the Cys^{73}-Cys^{73}, homodimeric form of Trx-1, which is the inactive state of Trx-1. Therefore, we hypothesized whether the interface of ADAM17/Trx-1 may also play a role in the Trx-1 activity.

Through different biochemical strategies, we have demonstrated in this study that (i) $ADAM17cyto^{WT}$ affects Trx-1 activity by increasing its disulfide reductase activity, its reduced state and its monomer state; (ii) the overexpression of $ADAM17cyto^{WT}$ or ADAM17 full-length increases the monomeric state of recombinant and endogenous Trx-1, respectively; (iii) lower cell oxidant levels and ADAM17 activity are observed in the presence of $ADAM17cyto^{WT}$ cells; and finally, (iv) ADAM17cyto may indirectly regulate other intracellular proteins. These data bring new insights into the role of ADAM17 in modulating indirectly the cell redox processes through Trx-1.

2. Results

ADAM17cyto mutant ($ADAM17cyto^{F730A}$) showed a decrease in the interaction with Trx-1, an increase in the oxidant levels, and a decrease in cysteine reactivity and redox activity when compared to $ADAM17cyto^{WT}$. Considering the evidences of the dimer and monomer forms of Trx-1 [24,28], we studied whether ADAM17 contributes with these states according to the described experimental design (Fig. 1).

In order to evaluate the role of ADAM17 interaction in the Trx-1 activity in the cell, we have generated a mutation of ADAM17 ($ADAM17cyto^{F730A}$) in which the amino acid substitution was predicted by *in silico* analysis to be important for the maintenance of the interacting interface [27]. According to the solid-phase binding assay, the interaction of Trx-1 decreased in the presence of $ADAM17cyto^{F730A}$ compared to $ADAM17cyto^{WT}$ (Fig. 2A).

To evaluate whether the interaction between Trx-1 and cytoplasmic domain of ADAM17 affected Trx-1 activity, several experiments were performed to address this effect. Firstly, we observed by a DTNB assay more reduced cysteines in Trx-1 in the presence of $ADAM17cyto^{WT}$ compared to $ADAM17cyto^{F730A}$ (Fig. 2B). Also, we observed that $ADAM17cyto^{WT}$ and $ADAM17cyto^{F730A}$ presented cysteine reactivity, showing higher reactivity in the former. Although these results indicate that $ADAM17cyto^{WT}$ may present more exposed cysteines than the mutant, we performed circular dichroism and no significant changes in the secondary structure and folding properties of these proteins were observed(Supplementary Figure 1). This difference between $ADAM17cyto^{WT}$ and $ADAM17cyto^{F730A}$ alone can be due to the protein flexibility [27].

Besides, we evaluated if $ADAM17cyto^{WT}$ could directly increase Trx-1 reducing activity upon Di-E-GSSG substrate. We first incubated Trx-1 with different $ADAM17cyto^{WT}$ and $ADAM17cyto^{F730A}$ protein concentrations (1, 2.5, and 5 μM) and the fluorescence resulted from the substrate reduction was measured. Fig. 2C shows that the concentration of $ADAM17cyto^{WT}$ above 2.5 μM was able to promote an increase in the substrate reduction ($p < 0.05$, Student's *t*-test), while $ADAM17cyto^{F730A}$ did not have this same effect on Trx-1 reducing activity. The results showed that in the presence of $ADAM17cyto^{WT}$, the reaction with the substrate was increased, compared to Trx-1 alone and Trx-1+$ADAM17cyto^{F730A}$, strongly suggesting that $ADAM17cyto^{WT}$ interaction with Trx-1 led the thiol reductase enzyme to a more active form.

To investigate whether ADAM17 binding was able to affect the catalytic and reductase activity of Trx-1, a cysteine reactivity assay was performed with $ADAM17cyto^{WT}$ and its mutant. To define the best concentration of H2O2 and Trx-1 used in this assay, a standard curve was performed (Supplementary Fig. 2A and B). A concentration of 10 μM H2O2 and 20 μg of Trx-1 was defined for all experiments (Supplementary Figure 2C). After incubation of the recombinant proteins with

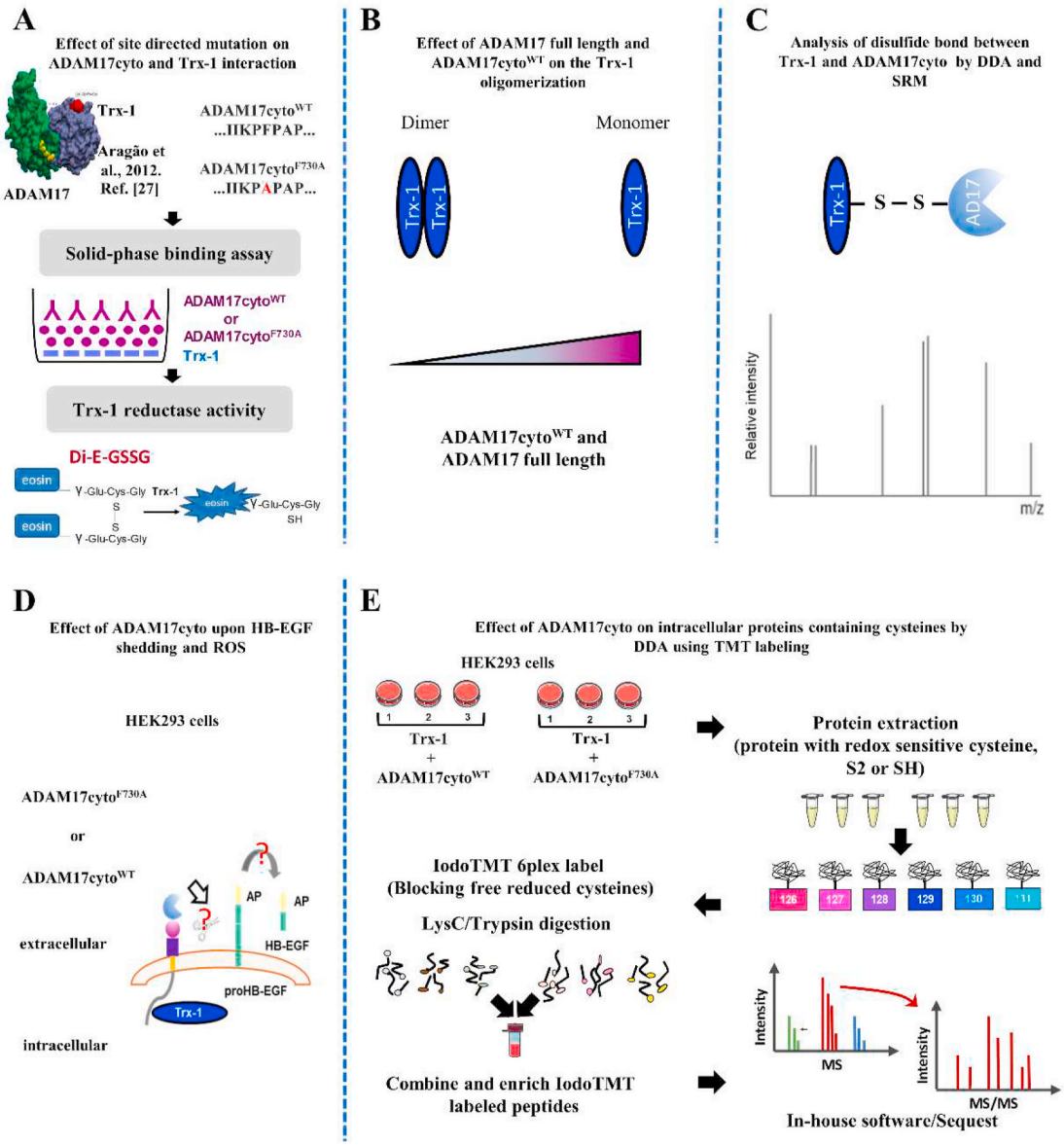

Fig. 1. Experimental design performed to identify the influence of ADAM17 upon Trx-1 reductive activity. A) Recombinant His-tagged proteins were expressed in BL21 cells and purified by affinity chromatography. Based on the *in silico* model of Trx-1-ADAM17 complex (Aragão et al., 2012), a mutation was generated in ADAM17cyto recombinant protein (ADAM17cyto^{F730A}) to evaluate the effect of ADAM17cyto^{F730A} in Trx-1 binding and its reductase activity. B) SDS-PAGE gel electrophoresis was performed followed by LC-MS/MS through band digestion to evaluate if ADAM17cyto^{WT} could increase the Trx-1 monomeric state. C) Data-dependent acquisition (DDA) and Selective Reaction Monitoring (SRM) were performed to detect the site responsible for homodimer formation between ADAM17cyto^{WT} and Trx-1. D) The ADAM17 shedding activity of HB-EGF-AP in HEK293 cells was measured by alkaline phosphatase enzymatic assay, while the effect of ADAM17 in hydrogen peroxide levels present in the extracellular medium of mammalian cells was analyzed by Amplex® Red assay. E) IodoTMT experiment was performed co-transfecting HEK293 cells with Trx-1 plus ADAM17cyto^{WT} or Trx-1 plus ADAM17cyto^{F730A}. Afterwards, protein quantification was performed by the BCA method and the cell lysate was mixed to iodoTMT six-plex isobaric label reagent set. Following, the proteins were digested, and the peptides enriched to perform *LC-MS/MS*. (For interpretation of the references to color in this figure legend, the reader is referred to the Web version of this article.)

H_2O_2 and Amplex Red® probe (Supplementary Figure 2), we detected more H_2O_2 consumption in the presence of Trx-1+ADAM17cyto^{WT} compared to Trx-1+ADAM17cyto^{F730A} or Trx-1 alone (Fig. 2D). Also to evaluate whether ADAM17cyto^{WT} modulated Trx-1 cysteine reactivity by interfering with the oxidation-reduction state of the catalytic site (Cys^{32}-Cys^{35}) or the dimeric state (Cys^{73}-Cys^{73}), the cysteine reactivity assay was performed with ADAM17cyto^{WT} and Trx-1 mutants (Trx-1^{K72A} and Trx-1$^{C32/35S}$). As expected, the activity of catalytic site mutant was not changed, but we showed that Trx-1^{K72A}, a catalytically inactive mutant due to its dimeric form [28], could have its cysteine reactivity increased by the incubation with ADAM17cyto^{WT}, suggesting the ability of ADAM17cyto^{WT} in the increase of Trx-1 activity acting upon the site of dimerization (Cys^{73}-Cys^{73}) (Fig. 2D).

ADAM17cyto^{WT} directly increased the monomeric state levels of Trx-1.

To evaluate whether ADAM17cyto^{WT} could increase the Trx-1 monomeric state, we next incubated recombinant Trx-1-HA protein with increasing concentrations of ADAM17cyto^{WT} (0, 3, 6, 12 μM). Then, the proteins were separated on a non-reducing SDS-PAGE and Coomassie Blue stained. Afterwards, the bands were digested with trypsin and evaluated by LC-MS/MS to perform the relative semi-quantification of peptides in the Trx-1 monomer and dimer bands (Fig. 3A). This result indicated that upon the increase of ADAM17cyto^{WT} concentration, there was an increase in Peptide Spectrum Matches

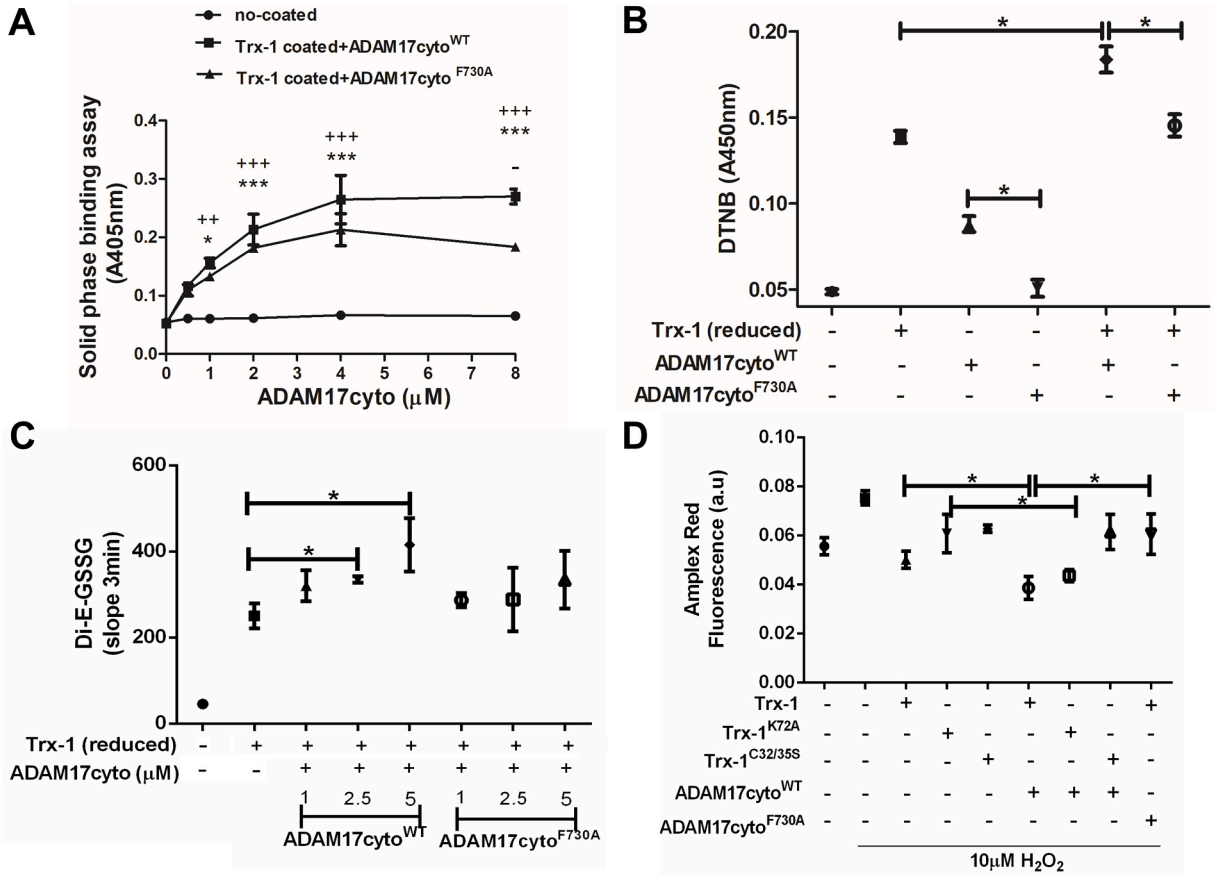

Fig. 2. The mutation in the interface of interaction of ADAM17cyto (ADAM17cyto^{F730A}) and Trx-1 disrupted their interaction and it affected Trx-1 reductase activity. A) Mutant ADAM17cyto^{F730A} bound less to Trx-1 than ADAM17cyto^{WT}. A solid-phase binding assay was conducted by adding 0–8 μM of either ADAM17cyto^{WT} or ADAM17cyto^{F730A} to 0.9 μM of immobilized Trx-1. Three independent experiments were performed in duplicate (two-way ANOVA followed by Bonferroni's posttest, $p < 0.05$). The plus (+) and asterisks (*) represent the statistics comparing the results from the no coated samples with Trx-1 coated + ADAM17cyto^{WT}, and Trx-1 coated + ADAM17cyto^{F730A}, respectively. The comparison between the samples Trx-1 coated + ADAM17cyto^{WT}, and Trx-1 coated + ADAM17cyto^{F730A} is represented by the minus symbol (−). Data are represented as mean ± SD. B) Trx-1 in the presence of mutant ADAM17cyto^{F730A} had less free cysteines than in the presence of ADAM17cyto^{WT}. DTNB assay was performed by incubating 20 μg of purified Trx-1 protein (previously reduced) with ADAM17cyto^{WT} or ADAM17cyto^{F730A} in the presence of DTNB. Three independent experiments were performed in duplicate (one-way ANOVA followed by Tukey's test $p < 0.05$). Data are represented as mean ± SD. C) Trx-1 in the presence of 2.5 μM of ADAM17cyto^{WT} had more reduced activity over Di-E-GSSG substrate. Di-E-GSSG substrate (150 nM) was incubated with 500 nM of purified and reduced Trx-1 alone, Trx-1/ADAM17cyto^{WT} or Trx-1/ADAM17cyto^{F730A} in a concentration-dependent manner, in 0.1 M potassium phosphate buffer with 1 mM EDTA pH 7.5 at 25 °C and the fluorescence (λex 545 nm and λem 520 nm) was measured over time and the slope of the curve was obtained. Three independent experiments were performed (Student's *t*-test $p < 0.05$). Data are represented as mean ± SD. D) Trx-1 in the presence of mutant ADAM17cyto^{F730A} had less cysteine activity than in the presence of ADAM17cyto^{WT}, while Trx-1^{K72A} mutant, that is inactive due to its dimeric form, in the presence of ADAM17cyto^{WT} had more cysteine reactivity. A cysteine reactivity assay was performed by incubating 20 μg of purified Trx-1 or Trx-1 mutant (Trx-1^{K72A} and Trx-1$^{C32/35S}$) proteins with ADAM17cyto^{WT} and Trx-1 with ADAM17cyto^{F730A} and 20 μM Amplex red and 1 U/mL peroxidase, followed by fluorescence measurements (λex 530 nm and λem 590 nm) and the addition of 10 μM of H_2O_2. Three independent experiments were performed in duplicate (one-way ANOVA followed by Tukey's test $p < 0.05$). Data are represented as mean ± SD.

(PSM) of Trx-1 in the respective Trx-1 monomer band, while decreased PSMs of Trx-1 in the related Trx-1 dimeric band (Fig. 3A, Supplementary Table 1).

To evaluate the propensity to dissociate the dimer in the presence of ADAM17cyto^{WT}, both recombinant proteins were incubated in a 1:1 ratio and analyzed by analytical ultracentrifugation. The sedimentation assays show that Trx-1 alone is formed mainly by dimers (~25 kDa, with large peak width), but in the presence of ADAM17cyto^{WT}, two distinct peaks could be observed, indicating monomeric Trx-1 and homo- and heterodimers of Trx-1 and ADAM17cyto^{WT} complex (Fig. 3B, Supplementary Table 2). Corroborating with the previous result, this result indicated that the addition of ADAM17cyto^{WT} changed Trx-1 conformation, favoring monomeric forms.

Next, we performed relative quantification of the peptide involved in the dimer disulfide bond by selective reaction monitoring (SRM) to confirm the formation of Trx-1 monomers in the presence of ADAM17cyto^{WT}. The peptides ^{73}CMPTFQFFK, *m/z* 574.76, +2 and ^{73}CM$_{ox}$PTFQFFK, *m/z* 603.27, +2 were monitored carbamidomethylated and with and without methionine oxidation. As a control, we spiked the synthetic labeled counterpart peptide (Supplementary Table 3). The results showed that the Cys^{73} containing peptides increased in the presence of ADAM17cyto^{WT}, in a concentration-dependent manner, suggesting an increase in Trx-1 monomeric state (Fig. 3C and Supplementary Table 4). We observed that ADAM17cyto^{F730A} followed a similar tendency, but with lower intensity due to the lower ability to bind Trx-1, as previously demonstrated (Fig. 2A).

ADAM17cyto^{WT} modulated the Trx-1 dimer and monomer ratio.

We next evaluated if the interaction between Trx-1 and ADAM17cyto^{WT} can be dependent on disulfide bond formation. For that, we evaluated the 30 kDa-dimer band indicated in Fig. 3A by data-dependent acquisition (DDA) at the four different ADAM17cyto^{WT} concentrations. We identified linked Trx-1 and cytoplasmic domain peptides (Fig. 4A). The Trx-1 peptide ^{73}CMPTFQFFK^{81} was linked with one trypsin missed cleavage ADAM17cyto peptide ^{816}VDSKETEC^{824} (*m/z* 813.83, +3) and

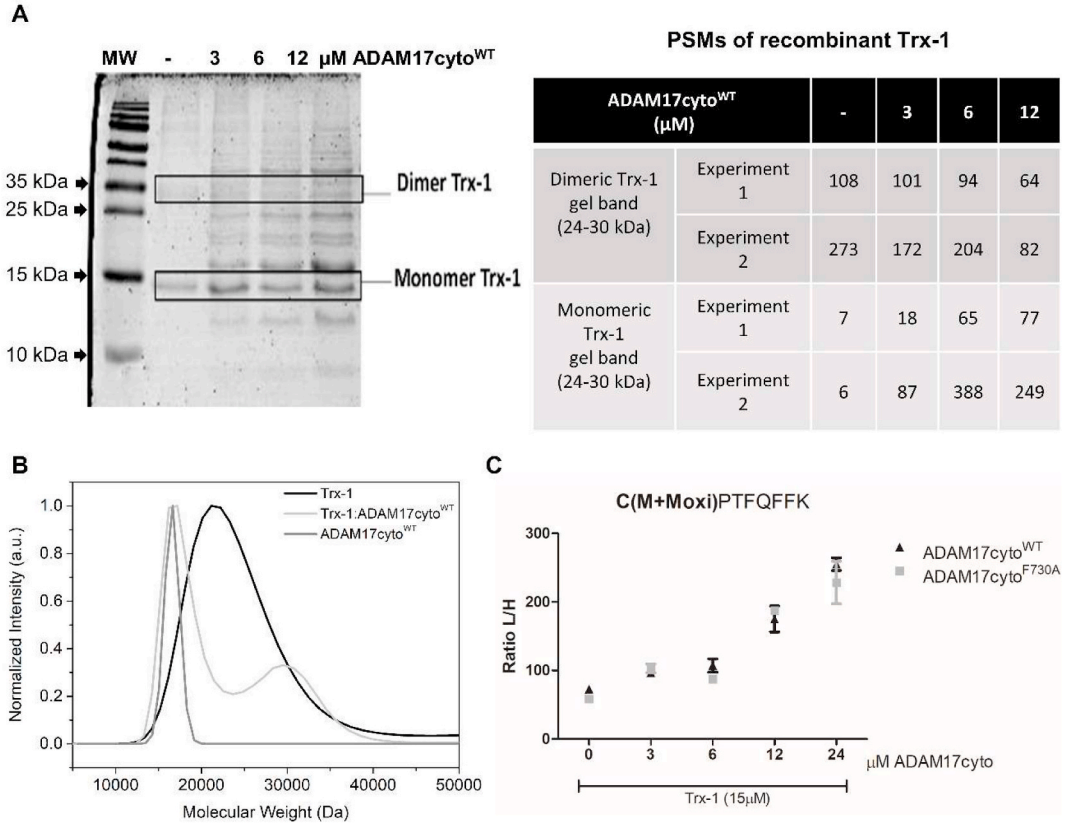

ADAM17cytoWT (μM)		-	3	6	12
Dimeric Trx-1 gel band (24-30 kDa)	Experiment 1	108	101	94	64
	Experiment 2	273	172	204	82
Monomeric Trx-1 gel band (24-30 kDa)	Experiment 1	7	18	65	77
	Experiment 2	6	87	388	249

Fig. 3. ADAM17cyto^{WT} modulated the Trx-1 dimer and monomer ratio. (A) Mass spectrometry analyses revealed an increase in the relative intensity of Trx-1 in the presence of increasing amounts of ADAM17cyto^{WT} (3, 6, 12 μM). The experiment was performed twice, with two different protein preparations. (B) Analytical ultracentrifugation data showed that the presence of ADAM17cyto^{WT} favored the monomeric state of Trx-1^{WT}. This experiment was performed four times with two different protein preparations. The x-axis below represents the molecular weight (MW) data from each sample and peak. (C) The carbamidomethylated peptide of Trx-1 C^{73} (C^{73}MPTFQFFK, *m/z* 574.76, +2 and C^{73}M$_{ox}$PTFQFFK, *m/z* 603.27, +2) was quantified by SRM. The peptide was measured in the absence of ADAM17cyto and in the presence of ADAM17cyto^{WT} and ADAM17cyto^{F730A} at concentrations of 3, 6, 12, and 24 μM. The proteins were submitted to in solution digestion in non-reduced conditions, with iodoacetamide treatment. For normalization of Trx-1 Cys^{73} peptide, the synthetic heavy labeled counterpart peptide was used. Data are represented as mean ± SD.

also with full-cleavage ADAM17cyto peptide ^{820}ETEC^{824} (*m/z* 813.83, +2). Note that Cys^{824} is the last amino acid in the ADAM17 sequence and Cys^{73} is the amino acid involved in Trx-1 dimer formation. All peptides involved in the same region, suggesting a disulfide bond shuffle between these proteins, were identified in the same band shown in Table 1, Supplementary Table 5 and Supplementary Figure 3. All the MS/MS spectra are shown in Supplementary Figure 4.

Furthermore, these heterodimer peptides were also monitored by SRM. The results indicated that the intensity of both peptides ^{73}CMPTFQFFK^{81} linked to ^{816}VDSKETEC^{824} and ^{73}CMPTFQFFK^{81} linked to ^{819}ETEC^{824} increases upon ADAM17cyto^{WT} and ADAM17cyto^{F730A} presence, in a concentration-dependent manner (Fig. 4B and C, Supplementary Table 6) and with lower intensity for ADAM17cyto^{F730A}.

We further evaluated if the interaction between Trx-1 and ADAM17cyto^{WT} was only dependent on the disulfide bond. For that, Trx-1 and ADAM17cyto^{WT} were treated with DTT, or DTT, and IAA or only IAA before recombinant protein incubations, followed by solid-phase binding assay. We observed higher interactions of ADAM17cyto^{WT} and Trx-1 in the absence of DTT, either in the absence or presence of IAA (Fig. 4D). It indicates that the interaction may happen independently of the disulfide bond. The SDS-PAGE performed in reducing and non-reducing conditions confirms the states of Trx-1 and ADAM17cyto upon DTT treatment (Fig. 4E).

ADAM17cyto^{WT} decreased cell redox state and ADAM17 shedding activity and increased Trx-1 monomeric levels in mammalian cells.

To investigate the effect of the ADAM17 modulation of Trx-1 in dimeric and monomeric forms on reactive oxygen species (ROS), we measured H_2O_2 levels by Amplex Red® probe in cells. Lower oxidant levels were detected when ADAM17cyto^{WT} and Trx-1^{WT} were co-expressed in HEK293 cells compared to ADAM17cyto^{F730A} and Trx-1 (Fig. 5A). Furthermore, we evaluated in the same conditions the consumption of H_2O_2 with the addition of 10 μM H_2O_2 into the system, besides Trx-1 alone. Similar results were found, in which the presence of ADAM17cyto^{WT} had higher consumption when compared to ADAM17-cyto^{F730A} (Fig. 5B). The ADAM17 sheddase activity was also evaluated in the presence of ADAM17cyto^{WT} or ADAM17cyto^{F730A}. Under PMA stimulation, in the presence of recombinant Trx-1 or Trx-1 + ADAM17cyto^{WT}, the shedding was reduced and the rescue was observed in the presence of Trx-1+ ADAM17cyto^{F730A} (Fig. 5C).

To investigate the conformational state of Trx-1 in cell lines in the presence of ADAM17, firstly, we co-overexpressed ADAM17cyto^{WT} and Trx-1 or ADAM17cyto^{F730A} and Trx-1 in HEK293 cells, pre-treated with 1 mM of H_2O_2 and evaluated in reducing and non-reducing conditions. The results showed a significant increase in the monomeric form of Trx-1 in the presence of ADAM17cyto^{WT}, indicated by the densitometry analysis (Fig. 5D).

The increase in the monomeric state of Trx-1 was also confirmed under endogenous levels of Trx-1. For this, we used HEK293/Flp-In ADAM17-HA cells overexpressing ADAM17 and we showed in Fig. 5E a pattern of higher abundance of the monomeric form of endogenous Trx-1. We also demonstrated in A431 ADAM17 knockdown cells the opposite results, indicating less abundance of the monomeric form of endogenous Trx-1 in ADAM17 knockdown cells (Fig. 5F). The transfection performed in all assays shown in Fig. 5 were performed following

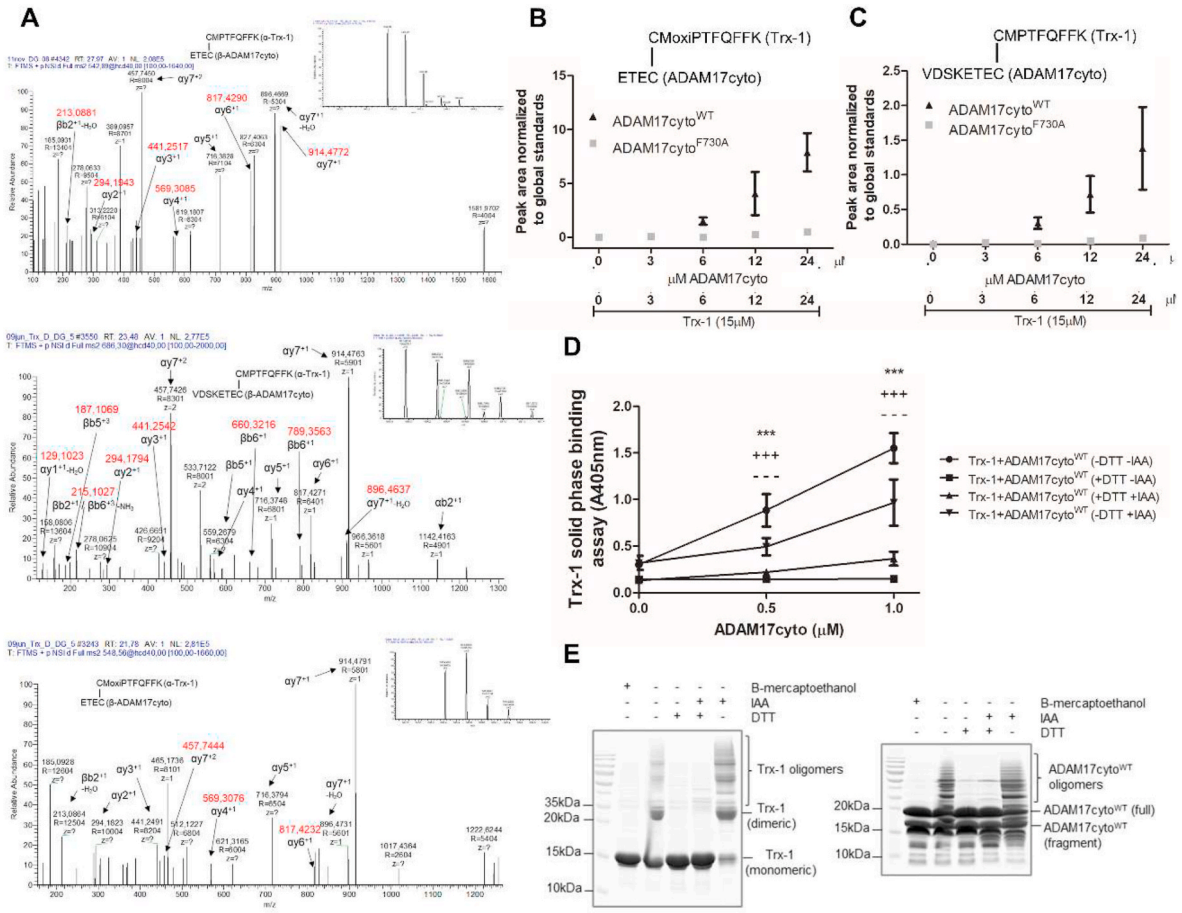

Fig. 4. One mechanism that ADAM17cyto^{WT} favored the monomeric state of Trx-1 is through disulfide bond formation. (A) Spectra of the peptides involved in the heterodimers (CMPTFQFFK-VDSKETEC, *m/z* 818.83, +3, and CMPTFQFFK-ETEC, *m/z* 813.83, +2) linked by a disulfide bond. Samples corresponding to 15 μM of Trx-1 recombinant protein in the presence of increasing amounts of ADAM17cyto^{WT} (3, 6, 12, and 24 μM) analyzed in non-reducing SDS-PAGE. The 30 kDa-band corresponding to the Trx-1 dimer size and/or Trx-1-ADAM17cyto^{WT} complex were excised, trypsin digested, and analyzed by mass spectrometry using DDA. The data were searched using MassMatrix and pLINK2 software. Two independent experiments were performed with 4 different ADAM17cyto concentrations and the disulfide bond peptide was identified in 2 conditions of each independent experiment in the presence of ADAM17cyto^{WT}. This experiment was repeated with two different sample preparations, and the same disulfide peptides were confirmed. The validation of the disulfide bond is shown. The symbol (−) represents the cysteines involved in disulfide bond formation. B–C) The disulfide bonds of the heterodimer Trx-1 and ADAM17cyto^{WT} (CMPTFQFFK-VDSKETEC, *m/z* 818.83, +3 and CMPTFQFFK-ETEC, *m/z* 813.83, +2) were quantified by mass spectrometry using SRM. The peptide corresponding to the disulfide bond was measured in the absence or presence of ADAM17cyto^{WT} and ADAM17cyto^{F730A} (3, 6, 12, and 24 μM). The experiment was performed in three technical replicates. Data are represented as mean ± SD. D) ADAM17cyto^{WT} bound more to Trx-1 in the absence of DTT and the presence of IAA treatments. A solid-phase binding assay was conducted by adding 0.5 and 1 μM of ADAM17cyto^{WT} to 0.9 μM of immobilized Trx-1. Four independent experiments, with two technical replicates, were performed (Two-way ANOVA followed by Bonferroni's posttest comparisons tests ($p < 0.05$)). The Trx-1 + ADAM17cyto^{WT} (-DTT -IAA) results were compared with Trx-1 + ADAM17cyto^{WT} (+DTT -IAA), Trx-1 + ADAM17cyto^{WT} (+DTT + IAA), Trx-1 + ADAM17cyto^{WT} (-DTT + IAA), and the statistics are represented by asterisk (*), plus (+) and minus (−) signals, respectively. Four independent experiments were performed. Data are represented as mean ± SD. E) 3 μg of recombinant proteins (Trx-1 and ADAM17cyto^{WT} complex and ADAM17cyto^{WT} alone) was loaded in a 15% SDS-PAGE gel followed by Western blot anti-ADAM17cyto. Samples were treated in the same conditions as in (E) and submitted to SDS-PAGE in non-reducing conditions using antibody against Trx-1 (left panel) or ADAM17cyto (right panel). One experiment was performed.

the same procedure as shown in Supplementary Figure 5A.

ADAM17cyto^{WT} was involved in the reduced state of intracellular proteins.

Considering the indirect or direct effect of Trx-1 monomer or dimer state in the global redox state, we evaluated the status of the reduced cysteine residues in proteins of HEK293 cells transiently expressing either ADAM17cyto^{WT} or ADAM17cyto^{F730A} by mass spectrometry using the labeling of cysteines through iodoTMT (Supplementary Fig. 5A-C and Supplementary Table 7).

2148 cysteine-containing peptides were identified, with 821 quantifiable peptides and 574 corresponding protein groups (filtered out after quality control). The results from Supplementary Fig. 5B and C showed the performance indicators, such as CV% indicating a reasonable quality control performance of the iodoTMT assay. The clustering analysis of iodoTMT data revealed that the peptide abundance of free cysteine residues was also able to separate the samples into two main clusters based on the expression of ADAM17cyto^{WT} or ADAM17cyto^{F730A} (Fig. 6A).

The volcano plot indicated the abundance of free cysteine residues, quantified by iodoTMT labeling, in which the majority of quantified peptides were more abundant in the Cys-SH state in Trx-1 + ADAM17cyto^{WT} compared to Trx-1+ ADAM17cyto^{F730A} by presenting the Cysred/Cysox fold change around 1.5 to 3 (Fig. 6B and Supplementary Figure 5D). Among the statistically significant abundant peptides, the identified peptides from proteins TXD17, CBR1, FAS, and PRDX1 showed peptides with reduced cysteines in the presence of ADAM17cyto. These proteins are particularly interesting due to their involvement in redox processes (Supplementary Table 8). Among the over-represented molecular functions were oxidoreductase functions (Fig. 6C, Supplementary Table 9 and Supplementary Table 10).

Table 1
Disulfide bond analysis in Trx-1 and ADAM17cyto^{WT} recombinant proteins by mass spectrometry using data-dependent acquisition. Intermolecular disulfide-linked peptides identified between Trx-1:ADAM17cyto^{WT}, Trx-1:Trx-1 and ADAM17cyto^{WT}:ADAM17cyto^{WT}.

Disulfide bond identified between Trx-1 and ADAM17cyto^{WT}	Trx-1	ADAM17cyto^{WT}	*m/z*, charge
Trx-1:ADAM17cyto^{WT}	$_{73}$CMPTFQFFK $_{81}$	$_{816}$VDSKETEC$_{824}$	685.96, +3$^{\#}$
	$_{73}$CMPTFQFFK$_{81}$	$_{820}$ETEC$_{824}$	813.83, +2$^{\#}$ 542.89, +3$^{\#}$
	$_{73}$CMoxiPTFQFFK$_{81}$	$_{820}$ETEC$_{184}$	548.22, +3$^{\#}$
	$_{73}$CMPTFQFFK$_{81}$	DDDDKC$_1$VDKKLDK$_8$	776.01, +3*
Trx-1:Trx-1	$_{22}$LVVVDFSATWCGPCK$_{36}$		811.89, +2*
	$_{73}$CMPTFQFFK$_{81}$:$_{73}$CMPTFQFFK$_{81}$		765.35, +3*
ADAM17cyto^{WT}: ADAM17cyto^{WT}		DDDDKC$_1$VDKKLDK$_8$:$_{820}$ETEC$_{824}$	672.28, +3*
		$_{816}$VDSKETEC$_{824}$: $_{816}$VDSKETEC$_{824}$	606.58, +3$^{\#}$

In bold are shown cysteines involved in disulfide bonds. All peptides were identified only in the 30-kDa SDS-PAGE band of Fig. 3A. Numbers in the sequences correspond to the first and last amino acids in the sequences of the recombinant proteins. The mass-to-charge ratios (*m/z*) of the precursor ions and their respective charge states are shown. The experiments were performed two times independently. The symbols indicate peptides identified in one (*) or two (#) independent experiments, considering all peptides identified by MassMatrix and pLINK2 together. When identified in one independent experiment, it was identified in at least 2 replicates. The MS/MS spectra for all disulfide bond peptides are shown in Figure S4.

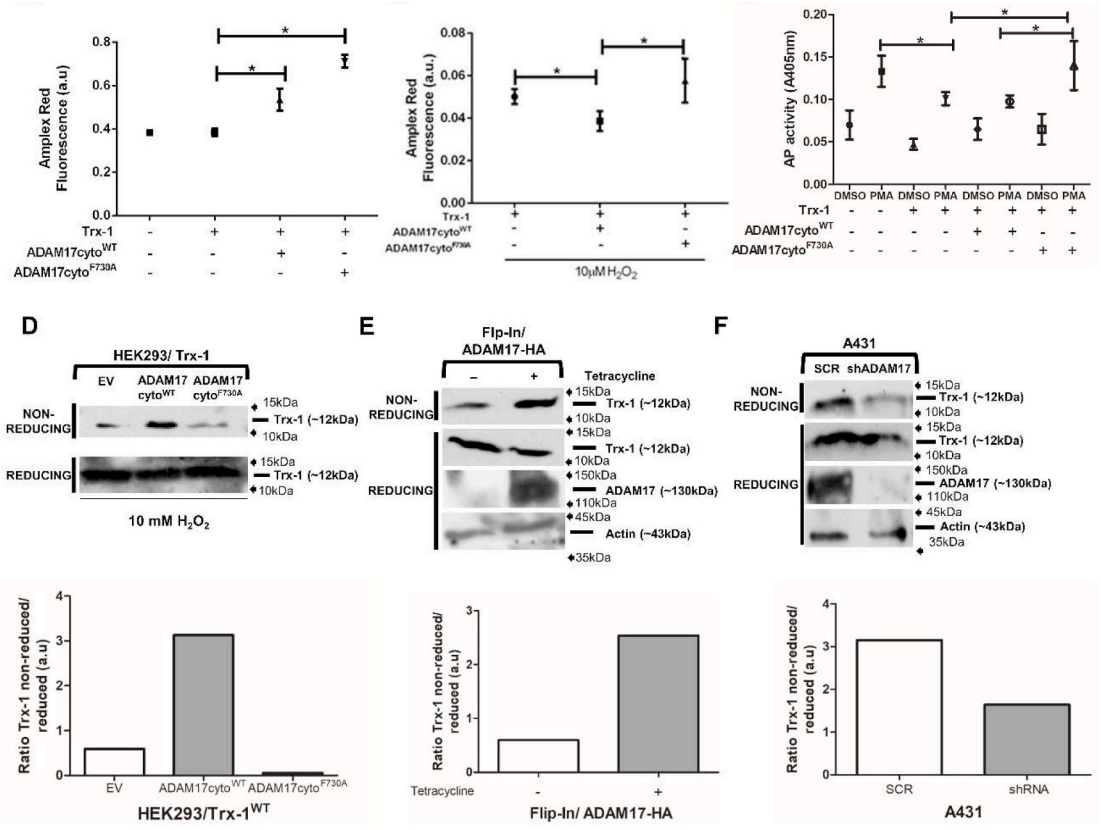

Fig. 5. ADAM17cyto^{WT} increased the redox activity in cells and stimulated HB-EGF shedding while the Trx-1 monomer form was favored in ADAM17cyto^{WT} and in ADAM17 overexpressing cells. A) Lower H_2O_2 levels were observed in ADAM17cyto^{WT} overexpressing cells compared to ADAM17cyto^{F730A}. HEK293 cells stably expressing AP-HB-EGF were transiently co-transfected with Trx-1/ADAM17cyto^{WT} or Trx-1/ADAM17cyto^{F730A} and stimulated with PMA. Cells were incubated with 20 μM Amplex Red and 1 U/mL of peroxidase, followed by fluorescence measurement (λex 530 nm and λem 590 nm). Three independent experiments were performed in duplicate (One-way ANOVA, followed by Tukey's multiple comparison posttest ($p < 0.05$)). Data are represented as mean ± SD. B) HEK293 cells overexpressing ADAM17cyto^{WT} had higher cysteine reactivity than overexpressing ADAM17cyto^{F730A}. A cysteine reactivity assay was performed using supernatants from HEK293 co-expressing Trx-1/ADAM17cyto^{WT} or Trx-1/ADAM17cyto^{F730A}, and incubating the supernatants with 20 μM Amplex red and 1 U/mL peroxidase, followed by fluorescence measurements (λex 530 nm and λem 590 nm) and hydrogen peroxide. Three independent experiments were performed in duplicate (One-way ANOVA followed by Tukey's test, $p < 0.05$). Data are represented as mean ± SD. C) Overexpression of ADAM17cyto^{WT} showed an inhibitory effect on ADAM17 shedding activity compared to ADAM17cyto^{F730A}. HEK293 cells stably expressing AP-HB-EGF were transiently co-transfected with Trx-1 and ADAM17cyto^{WT} or Trx-1 and ADAM17cyto^{F730A}, starved for 4 h and then stimulated with PMA, followed by measurement of alkaline phosphatase activity at 405 nm. Three independent experiments were performed in duplicate (One-way ANOVA followed by Tukey's test, $p < 0.05$). Data are represented as mean ± SD. D) The intracellular monomeric form of Trx-1 increased in the presence of ADAM17cyto^{WT}. Western blot under non-reducing conditions of HEK293 cells co-transfected with Trx-1 and ADAM17-cyto^{WT} or Trx-1 and ADAM17cyto^{F730A} and treated with 10 mM H_2O_2 for 10 min. This experiment was performed once. E) Reducing and non-reducing SDS-PAGE followed by Western Blots of endogenous Trx-1 in samples from HEK293/Flp-In cells overexpressing full-length ADAM17 showed an increase in the monomeric form of Trx-1. The monomeric form was normalized by the total amount of reduced Trx-1. This experiment was performed once. F) Reducing and non-reducing Western Blots of endogenous Trx-1 in scrambled and knockdown ADAM17 A431 cells showed a decrease in the monomeric form of Trx-1 in A431 scrambled cells. This experiment was performed once.

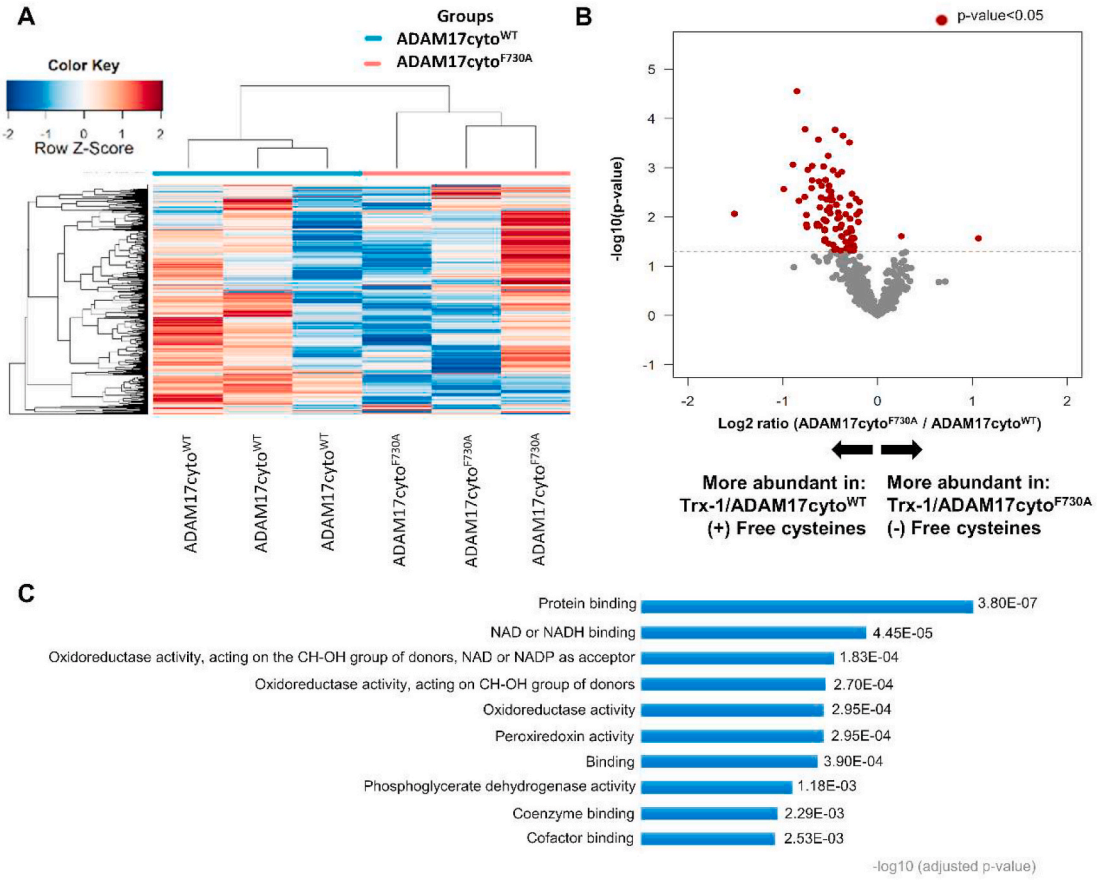

Fig. 6. ADAM17cyto^{WT} promoted an increase in the cysteine reduced state of several intracellular proteins. A) Clustering analysis of cysteine-containing peptides identified in Trx-1/ADAM17cyto^{WT} and Trx-1/ADAM17cyto^{F730A} samples (n = 3). Values for each peptide (rows) and each sample (columns) are colored based on the peptide abundance, in which high (red) and low (blue) values (*Z*-scored log2 LFQ intensity values) are indicated based in the color scale bar shown in the top left of the figure. The colored bars shown on the top of the figure indicate samples from the Trx-1/ADAM17cyto^{WT} cells (blue) or Trx-1/ADAM17cyto^{F730A} cells (pink). Hierarchical clustering was performed in the R environment using the Euclidean distance with the method Abscorrelation average. B) Volcano plot demonstrated that in the presence of ADAM17cyto^{WT}/Trx-1, the abundance of ninety-one peptides with free-cysteines, from a total of 2147 iodoTMT identified peptides, were increased compared to ADAM17cyto^{F730A}/Trx-1. Three independent experiments were performed (Student's *t*-test, $p < 0.05$). C) The 10 molecular functions that better represented the group of differentially reduced/oxidized proteins between Trx-1/ADAM17cyto^{WT} and Trx-1/ADAM17cyto^{F730A} were protein binding, NAD or NADH binding, oxidoreductase activity, peroxiredoxin activity, phosphoglycerate dehydrogenase activity, cofactor and coenzyme binding. (For interpretation of the references to color in this figure legend, the reader is referred to the Web version of this article.)

Finally, based on the present results, we propose that ADAM17 can regulate the balance between monomeric and dimeric states of Trx-1 with consequences in the intracellular and extracellular redox state of the cell and in the free cysteines of intracellular proteins (Fig. 7).

3. Discussion

Thioredoxin-1 and -2 are important antioxidant proteins that facilitate the reduction of proteins through cysteine thiol-disulfide exchange. It belongs to a system of redox molecules, including NADPH and the flavoprotein thioredoxin reductase (TrxR1). Trx-1 exists either in the reduced form Trx-$(SH)_2$ containing a dithiol, or in its oxidized form with an intramolecular disulfide bond between the Cys residues (Trx-S_2). Thus, Trx-1 participates in redox reactions through reversible oxidation of its active site. TrxR1 catalyzes the reduction of oxidized Trx-S_2 by NADPH using FAD and its active redox disulfide site. Then, Trx-$(SH)_2$ is capable to reduce the disulfide bond of various substrate proteins [29].

The structures of the reduced and oxidized human Trx-1 proteins (Trx-red and Trx-ox), and of the two mutant forms of the protein (Cys73/C73S; Cys32/Cys35) have been reported previously [24] showing dimeric thioredoxin in all four structures. Thioredoxin is thought to function as a monomer in redox reactions [24]. The role of disulfide bond formation in thioredoxin catalytic activity and oligomerization in non-redox conditions was assessed by previous studies [24]. In addition, an inactive dimeric form of human thioredoxin has previously been noted, leading to the suggestion that dimer formation may function in a regulatory sensor. That is plausible considering that oligomeric organization in crystallized proteins is not uncommon (eg. packing in *E. coli* thioredoxin crystals) [30]. Previous studies have been shown that Trx-1 noncatalytic cysteine residues were oxidized followed dimerization and inactivation of the enzyme, indicating that Cys73 is critical for the regulation of the enzyme activity via formation of intra- and inter-disulfide bonds [31], that were reduced by the enzyme with kinetics which supported a process of autoactivation. This maybe an important control mechanism for the activity of the bovine thioredoxin system and possibly other ortholog thioredoxins [32]. This reduced activity of Trx caused by dimerization provides a mechanism by which Trx activity is transiently inhibited under the conditions of oxidative stress, providing more time for sensing and transmission of oxidative signals. This can be seen by redox regulation of cellular PTEN activity, which is restrained by the oxidation of active-site cysteine by reactive oxygen species (ROS) [33]. Recovery of its enzymatic activity predominantly depends on the availability of cellular thioredoxin (Trx) and peroxiredoxins (Prx), both are important players in cell signaling. Trx and Prx undergo redox-dependent conformational changes through the oxidation of cysteine residues at their active sites. Their dynamics are

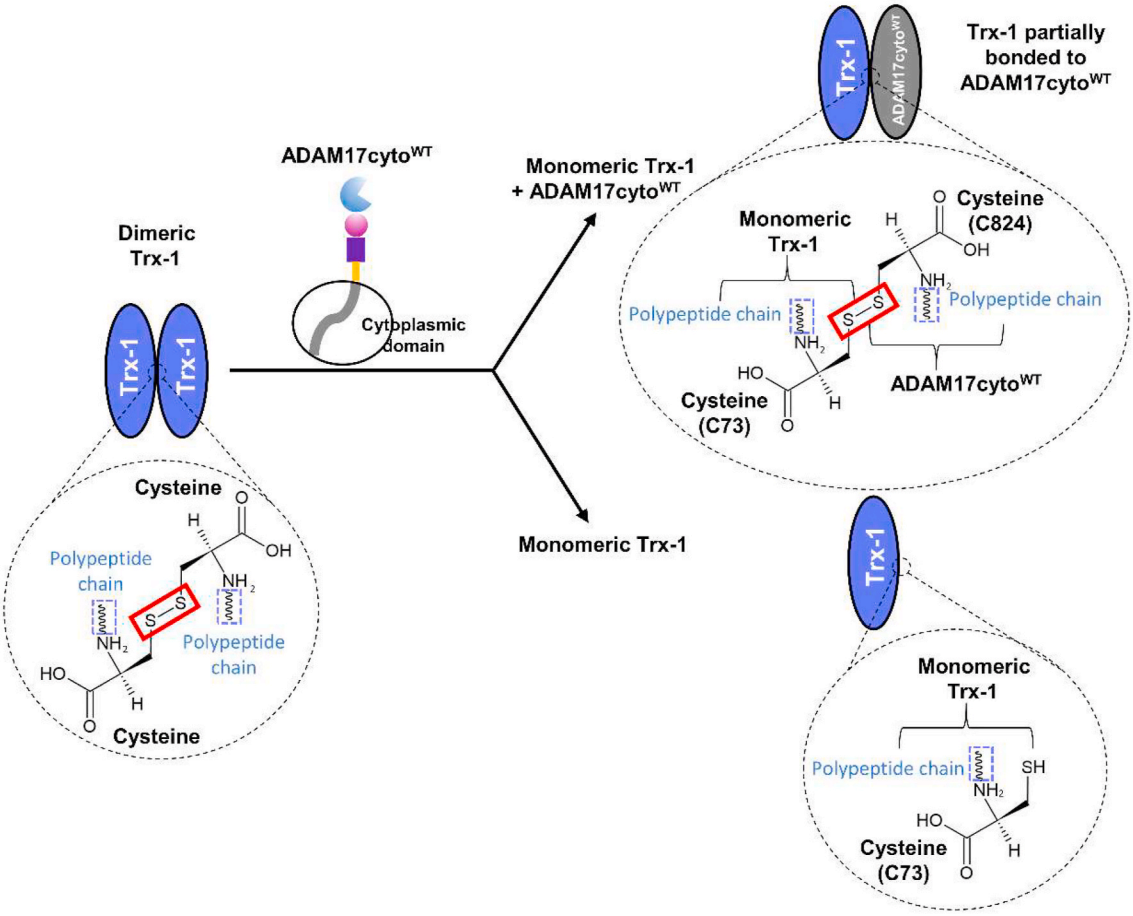

Fig. 7. Mechanism of interaction between the cytoplasmic domain of ADAM17 and Trx-1 led to conformation changes of Trx-1 and increased Trx-1 enzyme activity. The model showed that ADAM17cyto^{WT} positively regulated Trx-1 enzyme activity by favoring the Trx-1 monomeric state and it resulted in the increase of Trx-1 redox activity, promoting reduced state of intracellular proteins and lower H_2O_2 in the extracellular environment. One of the mechanisms that explained this dimer-monomer modulation by ADAM17cyto was the formation of a heterodimer with the disulfide bond formed between Cys^{824} of ADAM17cyto and Cys^{73} of Trx-1. Cys^{73} is known to be the site of Trx-1 dimerization [24].

essential for protein functionality and regulation. The same study shows a tight association of the redox regulation of PTEN with Trx dimerization and Prx hyperoxidation, providing guidance for the identification of novel therapeutic targets [33]. In the literature, there is an evidence of a dimeric Trx-1 structure, but the existence of a quaternary structure of this protein has been debated. In humans and other eukaryotes, the presence of a cysteine residue at the crystallographic symmetry axis points to the relevance of dimer formation in solution and *in vivo*. Crystallographic data for shrimp thioredoxin (*Lv*Trx) obtained under different redox conditions reveal a dimeric arrangement mediated by a disulfide bond through residue Cys73 and other hydrophobic interactions located in the crystallographic interface, as reported for human Trx [34]. Through the analysis of five mutants located at the crystallographic interface, the study provides structural and biochemical evidence for the existence in solution of monomeric and dimeric populations of wild-type *Lv*Trx and five mutants [34]. Based on the results of biochemical assays, SAXS studies, and the crystallographic structures it is clear that the Cys73 residue is essential for dimerization. Therefore, there are evidences of similar behavior in human thioredoxin, which shares a Cys at position 73 with *Lv*Trx, a structural feature that is also present in some Trxs from vertebrates and crustaceans [34]. However, how protein folding drives disulfide bond formation is poorly understood despite the role such proteins play in variety of extracellular and intracellular functions [35].

It is known that disulfide bonds are important stabilizing protein features as well as they can be considered labile cross-links promoted by disulfide shifts [36]. Although disulfide rearrangements through a thiol-disulfide exchange is recognized to play an important role in different physiological processes, its molecular determinants are still unknown. The reactivity of the thiol-disulfide exchange has been studied by computational models and in the case of thioredoxins, the hydrophobic pocket around the CXXC motif, the geometry, dynamics, and electrostatic environment are key elements to decide on the redox potential and kinetics of this family of enzymes [37]. The accessibility of the disulfide by the attacking thiol depends on the highly dynamic and steric protein composition, with or without an evolutionarily designed active site [38].

Besides PDI, it is already known that extracellular [39] and intracellular [27] thiol isomerases, such as, Trx-1 are potential regulators of ADAM17 [27,39]. We previously showed that Trx-1 interacts with the cytoplasmic domain of ADAM17 [27], where the interface of interaction is opposite to the catalytic site of Trx-1 and Trx-1 negatively modulates the activity of ADAM17. It is also known that Trx-1 can be modulated by a change in its dimeric/monomeric state since the dimeric form is inactive and does not expose the catalytic site [24]. Also, we imply that the effect that ADAM17cyto plays on Trx-1 dimerization can occur by promoting this conformational change and rendering the cysteines less accessible to dimerization and auto-regulation.

In the *in silico* ADAM17cyto and Trx-1 complex modeling, the residue F730 of ADAM17 was previously shown to be spatially located near the amino acid residue K72 of Trx-1, residue that was also shown to contribute to the binding interface and modeling of Trx-1 dimers (Cys^{73}-

Cys^{73}), disulfide bond in direct vicinity to K72) [27,28]. Therefore, we have interrogated if the interaction with ADAM17cyto^{WT} could modulate or influence the oligomerization state of Trx-1 and, thus, affect the oxidation/reduction state of the cell.

Herein, we have generated an ADAM17 mutation (ADAM17cyto^{F730A}) by site-directed mutagenesis to interfere in the interaction between ADAM17cyto and Trx-1. The residue F730 was chosen for mutation because *in silico* modeling revealed that it contributes to the complex binding energy and is predicted to be an important residue to maintain the complex [27].

Considering that the Trx-1 dimer is inactive and the Trx-1 Cys^{73} mutation is less prone to dimerization, Trx-1 activity could be regulated by modulating its dimeric/monomeric ratio [24]. It has been demonstrated that when the Cys^{73} residue is mutated, more Trx-1 homodimers are formed and the activity of Trx-1 is decreased [24]. Therefore, it is possible that this interaction interface may also regulate the balance between Trx-1 dimers and monomers, since a higher proportion of dimers compared to monomers could explain the lower activity of Trx-1. We propose that this regulation is performed by ADAM17cyto^{WT} or ADAM17 modulating the Trx-1 conformation and favoring the Trx-1 monomer state.

We indicated that the interaction of ADAM17cyto^{WT} with Trx-1 favors a monomeric form of Trx-1, with consequent higher activity and resulting in lower cell oxidant levels. In addition, we showed that one of the mechanisms of ADAM17cyto^{WT} can involve the disulfide bond formation between the proteins. Most importantly, the levels of the monomeric form of Trx-1 were also increased in ADAM17 overexpressing cells and decreased in ADAM17 knockdown cells.

On the other hand, as a control, ADAM17cyto^{F730A} was used as a consequence of its lower Trx-1 binding (Fig. 2A), and it was not able to increase the Trx-1 reductase activity (Fig. 2C), its presence promoted a higher hydrogen peroxide concentration (Figs. 2D and 5B) resulting in the increase of ADAM17 shedding activity compared with the wild type (Fig. 5C). The results indicated a constitutive shedding reduction by expression of recombinant Trx-1 and the rescue of shedding by ADAM17cyto^{F730A}. Also, these results reinforced that ADAM17cyto^{WT} directly and positively affected the Trx-1 redox activity. Besides, it corroborated with previous results showing that Trx-1 and reactive oxygen species modulated ADAM17 activity [28,40].

Besides, considering the role of the Trx-1 redox state, we evaluated the effect of ADAM17 on intracellular proteins, by iodoTMT analyses, using HEK293 cells co-transfected with Trx-1 and ADAM17cyto^{WT} or Trx-1 and ADAM17cyto^{F730A} (Fig. 6). The experiments suggested that the presence of ADAM17cyto^{WT} resulted in more free cysteine-containing enzymes and their substrates, involved in the redox pathway. For example, in the presence of ADAM17cyto^{WT}, peroxiredoxin-1 was identified in a more reduced form (LNCQVIGASVDSHFCHLAWVNTPK, m/z 550.46, +6, Supplementary Table 7). Also, TrxR1, known to reduce Trx-1, presented more free cysteines (CDYENVPTTVFTPLEYGACGLSEEK, m/z 856.67, +4, Supplementary Table 7), making it possible to regenerate Trx-1 in the presence of the complex with ADAM17cyto^{WT}. The modulation of thiol reductase activity by ADAM17cyto^{WT} reflected in the increase of the reduction state of several cysteine-containing proteins mainly associated with oxidoreductase function (Fig. 6C and Supplementary Table 8).

In the case of Trx-1, the Cys^{73} containing peptide was the unique peptide identified using iodoTMT labeling, and it was with reduced cysteine. However, the mass spectrometry analysis was not able to detect the differences in its abundance between the conditions, ADAM17cyto^{WT} or ADAM17cyto^{F730A}. We can suggest that although the iodoTMT labeling protocol performed an enrichment of peptides containing cysteines, possibly due to the high complexity of samples and untargeted approach, we could not quantify such small differences in cells (Supplementary Table 7).

On the other hand, the Cys^{73} containing peptide was identified by DDA and quantified by SRM (Fig. 3C) when we used recombinant proteins Trx-1 and ADAM17cyto. Moreover, we confirmed an increase in the free Cys^{73} containing peptides in the presence of concentration-dependent manner ADAM17cyto^{WT} (Supplementary Table 4), explaining the higher monomeric levels and active Trx-1. Corroborating with this result, these overall effects were reduced in the presence of ADAM17cyto^{F730A}. Together with this increase of the free Cys^{73} containing peptides, the heterocomplex of ADAM17cyto and Trx-1, linked by a disulfide bond (Fig. 4B and C), also increased in a concentration-dependent manner of ADAM17cyto^{WT}. Unfortunately, we were unable to confidently quantify the Cys^{73} containing homodimer peptides, due to the lower intensity of transitions resulted probably from the low accessibility of trypsin enzyme during digestion performed in non-reducing conditions.

The effect of ADAM17cyto^{WT} favoring the Trx-1 monomer state affects other free cysteine residue containing proteins, mostly involved in nucleotide binding and ligase activity, oxidoreductase activity, and peroxiredoxin activity (Supplementary Table 9) including carbonyl reductase [NADPH] (CBR1), isocitrate dehydrogenase [NAD] subunit alpha, mitochondrial (IDH3A) and thioredoxin domain-containing protein 17 (TXDC17). TXDC17, also known as TRP14 (thioredoxin-related protein 14), is a disulfide reductase with two active sites containing Cys residues in its WCPDC motif and it is known that Cys residues are also reduced by thioredoxin reductase (TRR) such as Trx-1 [41]. TRP14 is known to inhibit the TNF-α-induced NF-κB activation to a greater extent than Trx-1 [42]. Herein, we detected an increase in the reduced state level of TRP14 in the presence of ADAM17cyto^{WT}. This fact reinforces the complex nature of communication between ADAM17, Trx-1, and other TRR substrates, in addition to the cellular oxidant levels.

The signaling dependent on redox sensors in the cell is also known for other proteins. In non-oxidatively stressed cells, one of the MAPKKK (or MAP3K) enzymes named apoptosis signal-regulated kinase 1 (ASK-1) is kept inactive by association with reduced thioredoxin. Upon formation of a disulfide bond with thioredoxin via peroxiredoxin-catalyzed oxidation of two critical cysteines by H_2O_2, the oxidized thioredoxin dissociates from ASK-1 allowing its oligomerization and activation. The covalent binding of reduced Trx-1 to reduced ASK1 impairs its downstream activation of the kinases p38 and Jun NH2-terminal kinase (JNK). On the other hand, the oxidation of ASK1 promotes rapid multimerization [43]. H_2O_2 may also prolong MAP kinase signals by directly inactivating MAP kinase phosphatases via cysteine oxidation, and in growth factor signaling, oxidation of the phosphatase PTEN allows peptide growth factor (e.g. PDGF or EGF)-induced H_2O_2 production to mediate sustained proliferation signals [44].

Finally, it is interesting to note that the MS data-dependent acquisition indicated a disulfide shuffling within N-terminus and C-terminus of ADAM17cyto, and also within Cys^{73} of Trx-1 responsible for its homodimer (Table 1 and Supplementary Figure 4). A similar shuffling of disulfide bond patterns was previously observed in the membrane-proximal domain of ADAM17, controlled by the protein disulfide isomerase (PDI), resulting in an active open state and an inactive closed conformation [45,46].

Altogether, this study suggests a dynamic relationship between ADAM17 and Trx-1. Besides Trx-1 can negatively regulate ADAM17 activity [27], ADAM17cyto^{WT} and full-length ADAM17 can positively modulate Trx-1, thereby revealing a new and unexpected function for the cytoplasmic domain of ADAM17 promoting a dual regulation of the thiol reductase and as consequence an autoregulation of the metalloproteinase activity (Fig. 7). It has been suggested that strategies for increasing the antioxidant capacity of anti-tumor T cells, by activating Trx-1, can modulate their immune-metabolic phenotype leading to improved immunotherapeutic control of established tumors [47]. In this context, ADAM17cyto can be promoting a more antioxidant state, but there is also an increase of ADAM17 shedding.

These findings create a new paradigm for the influence of ADAM17 in regulating the redox state of the cells, implicating in novel mechanisms of ADAMs and their roles in redox regulation of the tumor

microenvironment.

4. Materials and methods

4.1. Chemicals and reagents

All chemicals were analytical grade obtained from commercial sources. Luria-Bertani (LB) broth, RPMI-1640 medium, sodium chloride (NaCl, 99%), calcium chloride dihydrate ($CaCl_2{\cdot}2H_2O$, 99%), hydrogen peroxide solution (H_2O_2, 30%), Tween-20 ($C_{58}H_{114}O_{26}$), 2,2′-Azino-bis (3-ethylbenzothiazoline-6-sulfonic acid) diammonium salt (ABTS, $C_{18}H_{24}N_6O_6S_4$, 98%), Triton X-100 (*t*-Oct–C_6H_4–$(OCH_2CH_2)_xOH$, x = 9–10), phenylmethylsulfonyl fluoride (PMSF, 98%), tetracycline ($C_{22}H_{24}N_2O_8$. xH_2O, 98%), hydrochloric acid (HCl, 37%), potassium chloride (KCl, 99%), anti-FLAG peroxidase (HRP, A8592), monoclonal anti-HA antibody (H3663), iodoacetamide (IAA, 99%), dithiothreitol (DTT, 99%), endoproteinase Lys-C sequencing Grade, 5,5′-dithiobis (2-nitrobenzoic acid) (DTNB, 99%), urea (NH_2CONH_2, pH 7.5–9.5), PMA ($C_{36}H_{56}O_8$, 99%), *p*-nitrophenyl phosphate disodium ($O_2NC_6H_4OP(O)(ONa)_2{\cdot}6H_2O$), diethanolamine ($HN(CH_2CH_2OH)_2$, 99%), HEPES (99.5%), magnesium chloride ($MgCl_2$, 98%), trifluoroacetic acid (CF_3COOH, 99%), trichloroacetic acid (Cl_3CCOOH, 99%), *cis*-2,6-Dimethylpiperidine ($C_7H_{15}N$, 98%), formic acid (HCOOH, 99%), acetonitrile (CH_3CN, 99.8%), and tetraethylammonium bicarbonate ($(CH_3CH_2)4\ N(HCO_3)$, 95%) were purchased from Sigma-Aldrich. Penicillin, streptomycin, and trypsin were purchased from Invitrogen. Ethylenedinitrilotetraacetic acid disodium salt dihydrate (EDTA, 0.5 M pH 8), DMEM medium, FBS, and geneticin 418 were purchased from Gibco. Imidazole ($C_3H_4N_2$, 99%) was purchased from Oakwood Chemical. Citric acid ($C_6H_8O_7{\cdot}H_2O$, 99.5–100%), sodium phosphate dibasic (Na_2HPO_4, 99%), and potassium dihydrogen phosphate (KH_2PO_4, 99.5–100%) were purchased from Merck. Isopropyl-β-*d*-thiogalactopyranoside (IPTG, 99%) was purchased from Promega. Tris (hydroxymethyl)-aminomethane (Tris, $NH_2C(CH_2OH)_3$, 99.8%) was purchased from Affymetrix. The cocktail Protease Inhibitor was purchased by Roche. The TMT10plex™ isobaric label reagent set was purchased from Thermo Fisher Scientific. The antibody *anti*-Trx (LF-PA0187) was purchased from AbFrontier and the anti-actin (ab8227) was purchased from Abcam.

4.2. Cell culture and transient transfections

HEK293 cells were cultured in DMEM medium supplemented with 10% FBS, 100 IU/mL penicillin, and 100 mg/mL streptomycin, at 37 °C in a humidified atmosphere with 5% CO_2. HEK293 stably expressing alkaline phosphatase reporter (HB-EGF-AP) were cultured in DMEM medium supplemented with 10% FBS, 100 IU/mL penicillin, and 100 mg/mL streptomycin at 37 °C in a humidified atmosphere with 5% CO_2. The geneticin 418 (G418) antibiotic was added to the culture medium (1 mg/mL final concentration) to maintain the selection of the clone. HEK293/Flp-In ADAM17-HA cells were cultured in DMEM medium supplemented with 10% FBS, 100 IU/mL penicillin, and 100 mg/mL streptomycin, at 37 °C in a humidified atmosphere with 5% CO_2. Tetracycline was added to the culture medium (1 μg/mL final concentration) to induce the expression of the ADAM17-HA recombinant gene for 24 h at 37 °C. The A431 ADAM17 knockdown cells) were cultured in RPMI-1640 medium supplemented with 10% FBS, 100 IU/mL penicillin, and 100 mg/mL streptomycin, at 37 °C in a humidified atmosphere with 5% CO_2. The geneticin 418 (G418) antibiotic was added to the culture medium (1 mg/mL final concentration) to maintain the selection of resistant cells. Cells were cultured until 70–80% of confluency.

Mutagenesis of ADAM17cyto (ADAM17cyto^{F730A}) was performed with the mutagenesis kit (Stratagene, San Diego, CA) and specific primers were used (Forward: 5′-GTTCGCATTATCAAACCCGCTCCTGCGCCCCAG-3′ and Reverse: 5′-CTGGGGCGCAGGAGCGGGTTTGATAATGCGAAC-3′), following the manufacturer's protocol. ADAM17cyto^{F730A} was cloned in pET28a (+) and pcDNA 3.1+, for protein expression in *E. coli* and mammalian cells, respectively. Trx-1, ADAM17cyto^{WT} and Trx1 mutants containing plasmids for protein expression in *E. coli* and mammalian cells have been previously described [27]. For *E. coli* expression, genes for Trx-1 and Trx-1 mutants (Trx-1^{K72A} and Trx-1$^{C32/35S}$) were cloned with a HIS6 tag in the N-terminal and an HA tag in the C-terminal; genes for ADAM17cyto^{WT} and ADAM17cyto^{F730A} were cloned with a HIS6 and FLAG tags in the N-terminal. For expression in mammalian cells, genes for Trx-1 and Trx-1 mutants (Trx-1^{K72A} and Trx-1$^{C32/35S}$) were cloned with an HA tag in the C-terminal; genes for ADAM17cyto^{WT} and ADAM17cyto^{F730A} were cloned with a FLAG tag in the N-terminal. HEK293 was transiently transfected by Lipofectamine, following the manufacturer's protocol (Invitrogen, Carlsbad, CA) or using polyethylenimine (Polysciences Inc., Warrington, PA) for 48 h.

4.3. Expression and purification of Recombinant His-tagged proteins

Trx-1, Trx-1^{K72A}, Trx-1$^{C32/35S}$, ADAM17cyto^{WT} and ADAM17cyto^{F730A} proteins were expressed in BL21 (DE3) cells at 37 °C for 4 h after induction with 0.5 mM IPTG in LB. The harvested cells were resuspended in lysis buffer (20 mM Tris, pH 7.5, containing 1 mM $CaCl_2$ and 1 mM PMSF) and disrupted by lysozyme treatment (100 μg/mL for 30 min on ice), followed by sonication (Vibracell VCX 500; Sonics & Materials, Inc., Newtown, CT). The suspensions were centrifuged at 20,000×*g* for 10 min at 4 °C. The supernatant was loaded onto nickel-charged 5-mL His Trap Chelating columns (GE Healthcare, Chicago, IL) using a flow rate of 1 mL/min in buffer A (20 mM Tris, pH 7.5, containing 1 mM $CaCl_2$ and 1 mM PMSF). Proteins were eluted using a linear gradient of 0–1 M imidazole. All the purified fractions were combined in a 3-kDa cut-off Amicon filter (Millipore, Burlington, MA) and the buffer was changed into phosphate-buffered saline (PBS). PBS was prepared with NaCl (137 mM), KCl (2.7 mM), Na_2HPO_4 (10 mM), and KH_2PO_4 (1.8 mM), the pH was adjusted to 7.2 with HCl for 1 L of an aqueous solution. The purified fractions were separated by 15% SDS-PAGE under denaturing conditions to evaluate the quality of the protein purification. Trx-1^{K72A} and Trx-1$^{C32/35S}$ were purified as previously reported [28]. Final protein concentration was determined by a Bicinchoninic acid (BCA) protein assay kit (Thermo Fisher Scientific, Waltham, MA). At least three independent preparations of purified protein were obtained for further experiments.

4.4. Solid-phase binding assay

One μg of purified Trx-1 was immobilized into a 96-well polystyrene High Bind microtiter plate (Corning Glass, Corning, NY) in a 0.1 M sodium carbonate buffer, pH 9.6, with gentle agitation overnight at 4 °C, as described previously [48]. The wells were washed three times with wash solution (PBS supplemented with 0.05% Tween 20) and then blocked with PBS containing 5% nonfat dry milk for 2 h at room temperature. After blocking, the wells were washed again and the purified proteins, ADAM17cyto^{WT} and ADAM17cyto^{F730A}, were added in an increasing concentration (0.5–8 μM), diluted in PBS supplemented with 0.05% Triton X-100 and 0.1% BSA. The plates were incubated for 2 h at room temperature and after that, the wells were washed three times. We incubated the complexes for 1 h at room temperature with anti-FLAG peroxidase-linked antibody, diluted at 1:5000 for 1 h at room temperature. After incubation with the antibody, the wells were washed three times and a buffer containing 2,2′-azinobis-(3-ethylbenzothiazoline-6 sulfonic acid, 0.1 M citric acid, and 0.03% H_2O_2 was added. We detected the protein binding using a colorimetric ELISA assay. The absorbance was measured in a plate reader at Aλ 405 nm. Three independent experiments were performed. For dithiothreitol (DTT) or/and iodoacetamide (IAA) treatment, the same protocol was performed but in this case both Trx-1 and ADAM17cyto^{WT} were previously treated with 5 mM DTT for 15 min and 14 mM IAA for 30 min at room temperature, with the

purpose to reduce and block the free cysteines, respectively, before adding the proteins into the 96 well plate. Four independent experiments were performed in two technical replicates.

4.5. Assays for measuring reactivity of cysteines

To measure the reactivity of cysteines in HEK293 cells extracellular medium, upon the presence of Trx-1/ADAM17cyto^{WT} complex, we measured the consumption of H_2O_2 in the secretome of co-expressing Trx-1/ADAM17cyto^{WT} or Trx-1/ADAM17cyto^{F730A} cells. The indirect measurement of cysteine reactivity was performed as described previously [28]. First, the secretome of co-transfected cells was placed into a 96 well-plate with 100 μM Amplex® Red reagent (Invitrogen, Carlsbad, CA), 0.2 U/mL HRP and 10 μM H_2O_2 in 1x reaction buffer. To measure the direct effect of the complex in the reactivity of Trx-1 recombinant cysteines, we measured the H2O2 levels by incubating the purified proteins in the specified concentrations into a 96 well-plate with 20 μM Amplex® Red reagent, 0.2 U/mL HRP and 10 μM H_2O_2 in 1x reaction buffer. All reactions were measured in a fluorimeter at λex of 530 nm and λem of 590 nm. To define the best concentration of H_2O_2 and Trx-1 used in this assay, three independent experiments were performed. Also, three independent experiments in triplicate were performed for recombinant proteins and three independent experiments in duplicate were performed for HEK293 cells.

Also, the DTNB assay was performed to evaluate the reactivity of Trx-1 recombinant cysteines in the presence of the complex with ADAM17cyto as described previously [28]. For that, recombinant Trx-1 was incubated with DTT (10 mM) and excess DTT was removed by buffer exchange in Microcon® Filter (Merck, Darmstadt, DE). 5 μL of 10 mM DTNB (at a final concentration of 1 mM) was added to 100 μM of recombinant, purified, and previously reduced Trx-1^{WT} together with ADAM17cyto^{WT} or ADAM17cyto^{F730A} in 43 μL of 100 mM of glycine buffer at pH 8.3. The reaction product was measured at 450 nm. Three independent experiments were performed. Besides, to evaluate if the mutation in ADAM17cyto was able to change its secondary structure, circular dichroism analysis was performed with both proteins (ADAM17cyto^{WT} and ADAM17cyto^{F730A}) as previously described [49]. One independent experiment was performed.

4.6. Reduction of Di-E–GSSG by Trx-1

To test whether ADAM17cyto^{WT} could affect Trx-1 reducing activity and determine the concentration of ADAM17cyto^{WT} and ADAM17cyto^{F730A} that should be used in the assay, increasing concentration of the proteins (1, 2.5 and 5 μM) were incubated with 500 nM of previously reduced Trx-1 and 150 nM of Di-E–GSSG in 0.1 M potassium phosphate buffer with 1 mM EDTA pH 7.5 (PE buffer) at 25 °C. Later, fluorescence was measured at λex of 525 nm and λem of 545 nm for all assays over time. The experiment was performed three times independently in duplicate.

4.7. Assessment of Trx-1 oligomerization by mass spectrometry using data-dependent acquisition (DDA)

To analyze the monomeric state of Trx-1, recombinant purified Trx-1 (15 μM) and ADAM17cyto^{WT} (3, 6, 12, and 24 μM) proteins were first incubated together for 30 min on ice. Furthermore, sample buffer (without β-mercaptoethanol) was added to the protein complex and monomer and dimer forms of the recombinant protein Trx-1 alone or incubated with ADAM17cyto^{WT} was analyzed on a non-reducing 15% SDS-PAGE gel. This experiment was performed two times.

In parallel, to perform the relative semiquantitative analysis of recombinant Trx-1 protein in the monomer and dimer forms the peptide spectrum matches (PSMs) were obtained. For that, gel bands were analyzed from a non-reducing 15% SDS-PAGE gel and the bands of monomer and dimer forms in Trx-1 alone or incubated with ADAM17cyto^{WT} were first alkylated (14 mM iodoacetamide, 30 min at room temperature in the dark), and then digested with trypsin (Promega, Madison, WI). The samples were dried in a vacuum concentrator and reconstituted in 20 μL of 0.1% formic acid. Four and a half microliters of the resulting peptide mixture were analyzed on an LTQ Orbitrap Velos mass spectrometer (Thermo Fisher Scientific, Walthan, MA) coupled with LC-MS/MS by an EASY-nLC system (Proxeon Biosystem, Odense, DK) through a Proxeon nanoelectrospray ion source according to Ref. [27].

Peak lists (msf) were generated from the raw data files using Proteome Discoverer version 1.4 (Thermo Fisher Scientific) with the Sequest search engine and searched against the Human Uniprot database concatenated with the recombinant Trx-1 and ADAM17cyto^{WT} protein sequences (95,544 sequences; 38, 079, 025 residues, released in May 2019). The search included carbamidomethylation (+57.021 Da) and oxidation of methionine (+15.995 Da) as variable modifications; one trypsin missed cleavage and a tolerance of 10 ppm for precursor and 0.02 Da for fragment ions (Supplementary Table 1). The false discovery rate (FDR) was calculated at 1%. A target–decoy search strategy approach was used to estimate the false-positive discovery rate [50]. This experiment was performed twice, with two different protein preparations.

The same samples were also analyzed regarding the presence of Trx-1/ADAM17 disulfide bond formation. For that, the raw data files generated by Xcalibur version 2.1 (Thermo Fisher Scientific, Watlham, MA) were converted to a peak list format (mgf) by using Proteome Discoverer version 1.4 (Thermo Fisher Scientific, Watlham, MA). The mgf files were analyzed in MassMatrix version 3.10 and pLINK2 version 2.3.6 to automatically search disulfide bonds against databases containing the Trx-1^{WT} and ADAM17cyto^{WT} sequences, according to the software instructions. The parameters for disulfide analysis used in MassMatrix and pLINK2 software were oxidation of methionine (+15.995 Da) as variable modification, three trypsin missed cleavages, and a tolerance of 20 ppm for precursor and 20 ppm for fragment ions. Search results with high confidence and potential disulfide cross-linked peptides were manually validated for b and y ion series containing y and b chains [51,52]. This experiment was performed two times, with two different protein preparations (Table 1 and Supplementary Table 5).

4.8. Analytical ultracentrifugation of Trx-1/ADAM17cyto^{WT} and Trx-1/ADAM17cyto^{F730A} complexes

Sedimentation velocity experiments for ADAM17cyto^{WT}, Trx-1, and complexes formed by ADAM17cyto^{WT}/Trx-1 were performed in a BeckmanCoulter OptimaTM XL-A (Beckman Instruments Inc. Palo Alto, CA) ultracentrifuge at 10 °C, and samples rotated at 40,000 rpm with Aλ monitoring at 280 nm. This experiment was performed four times independently.

In the condition ADAM17cyto^{WT}/Trx-1, the ADAM17cyto^{WT} was incubated together with Trx-1 for 15 min at room temperature (R.T), before ultracentrifugation, to allow the complex to be formed. Consecutive scans were automatically recorded at regular intervals and data was analyzed with the software Sedfit Schuck P 2000 Size distribution analysis of macromolecules by sedimentation velocity ultracentrifugation and Lamm equation modeling (Supplementary Table 2) [53].

4.9. Quantitative analysis of Trx-1 Cys^{73} reduced and oxidized state in the presence of ADAM17cyto^{WT} and ADAM17cyto^{F730A} by mass spectrometry using selective reaction monitoring (SRM)

To evaluate the effect of ADAM17cyto^{WT} and ADAM17cyto^{F730A} on Trx-1 Cys^{73} reduced state, the Trx-1 peptide (^{73}CMPTFQFFK^{81}), which contains the cysteine residue responsible for Trx-1 homodimerization, was submitted to relative quantification using SRM as previously described in Ref. [28], with modifications. After the proteins' incubations (Trx-1+ ADAM17cyto^{WT} and Trx-1+ ADAM17cyto^{F730A},

under ADAM17cyto concentrations of 3, 6, 12, and 24 μM) during 15 min at 25 °C, all reactions were stopped by denaturing condition using 4 M urea, in non-reducing conditions. The mixture of proteins was alkylated and submitted to trypsin digestion (1:50). The experiment was performed in three technical replicates.

Proteotypic peptides for Trx-1 and ADAM17cyto proteins were selected based on our DDA analysis and following the rules as previously described [53,54]. Briefly, a total of 3 proteotypic peptides were selected to be monitored label-free, including the disulfide-linked peptide at position Cys^{73}, and a total of 2 proteotypic peptides were selected to be monitored label-based, including the carbamidomethylated peptide at position Cys^{73} with and without methionine oxidation (Supplementary Table 3). At least five transitions were monitored for the light and heavy peptides, with a total of 90 transitions. A mixture of 2 pmol of the heavy isotopic labeled peptide was added to the samples prior to desalinization performed using Sep-pak C18 cartridge (Waters, Milford, MA). Internal retention time standards (iRT, Pierce Peptide Retention Time Calibration Mixture, Thermo Fisher Scientific, Watlham, MA) were spiked in all samples at 50 fmoL/μl, before sample injection and four peptides with 12 transitions were monitored. Also, two trypsin auto-lysis peptides were monitored to evaluate the trypsin digestion efficiency.

Samples were analyzed on a Xevo TQ-XS triple quadrupole mass spectrometer (Waters, Milford, MA) equipped with an electrospray ion source (Ion Key; Waters) and using MassLynx software (version 4.2) as previously described [28]. Visualization and inspection of peaks were manually performed in Skyline. The label-free and label-based quantification had the light peptides checked regarding the quality of data by observing co-elution of all five transitions and relative intensity correlation with spectral library (dotp) and stable isotope-labeled peptides (SIL) (rdotp). For label-based quantification, the light peptides were normalized using SIL (Supplementary Table 4) and for label-free quantification, the light peptides were normalized to the intensity of two iRT peptides (average intensity value was used as denominator) (Supplementary Table 6). iRT peptides intensities were also evaluated among all runs to determine the quality of the LC. In addition, in the case of methionine-containing peptide, the intensity of the two forms, oxidized or non-oxidized, were summed (Supplementary Tables 4 and 6). In addition, for label-free disulfide bond peptides, the transitions were selected based on the inspection of MS/MS spectra provided by DDA.

4.10. Measurement of extracellular H_2O_2 levels

To measure the effect of $ADAM17cyto^{WT}$ in hydrogen peroxide levels present in the extracellular medium of mammalian cells, Amplex Red Hydrogen Peroxide/Peroxidase Assay Kit® (Molecular Probes, Invitrogen, Carlbad, CA) was used according to the manufacturer's protocol and the reaction was read in a fluorimeter at 37 °C, at λex of 530 nm and λem of 590 nm. Briefly, HEK293 cells stably transfected with HB-EGF-AP were seeded (0.3×10^6) into 6-well plates (Corning, Corning, NY) and starved for 24 h. Next, the cells were transiently co-transfected for 6 h with the encoding vectors Trx-1/$ADAM17cyto^{WT}$ or Trx-1/$ADAM17cyto^{F730A}$. After, cells were activated with PMA (50 ng/mL) for 30 min in DMEM (without FBS), they were harvested, washed with cold PBS and trypsinized. Approximately, 1×10^4 cells were placed into a 96-well microplate and to the cells was added 50 μL of the reaction buffer (working solution of 20 μM Amplex® Red reagent, 0.2 U/mL HRP and 1x reaction buffer) to each well. The cells were incubated in the dark for 30 min and the reaction was measured in the fluorimeter. Three independent experiments in duplicate were performed.

4.11. Analysis of ADAM17 activity

To measure ADAM17 shedding activity in HEK293 cells, upon the presence of Trx-1WT/ADAM17cytoWT complex, HEK293 cells stably transfected with HB-EGF-AP [27] were seeded (0.3×10^6) into 6-well plates (Corning, Corning, NY). The following day, the cells were transiently transfected for 24 h with vectors encoding Trx-1, $ADAM17cyto^{WT,}$ and $ADAM17cyto^{F730A}$ for co-expression of Trx-1/$ADAM17cyto^{WT}$ or Trx-1/$ADAM17cyto^{F730A}$. After 24 h, the cells were trypsinized, counted, and 3×10^5 cells were seeded into 24-well plates (Corning, Corning, NY). The following day, the cells were starved for 4 h. Following starvation, the cells were activated with PMA (50 ng/mL) [54] for 1 h in a phenol-free medium. The conditioned media was removed from the culture plate and the shedding of HB-EGF-AP was measured by alkaline phosphatase enzymatic assay. Briefly, 100 μL of conditioned media was collected from each well and added to individual wells of a 96-well plate containing 100 μL of AP buffer (0.5 M Tris-HCl, pH 9.5, containing 5 mM *p*-nitrophenyl phosphate disodium, 1 mM diethanolamine, 50 μM $MgCl_2$, 150 mM NaCl, 5 mM EDTA). After the enzymatic reaction was completed the product was measured at an absorbance wavelength (Aλ) of 405 nm. Three independent experiments were performed in duplicate for non-oxidative and oxidative conditions.

4.12. Analysis of conformational state of Trx-1 by Western blot

To analyze if $ADAM17cyto^{WT}$ is able to alter Trx-1 conformation in mammalian cells, Trx-1 with $ADAM17cyto^{WT}$ or $ADAM17cyto^{F730A}$ were co-expressed in HEK293 cells for 48 h, followed by cell lysis with lysis buffer (50 mM Tris-HCl pH 7,4, 150 mM NaCl, 1 mM EDTA, 1% Triton and protease inhibitor cocktail tablet with the addition of 100 mM iodoacetamide) [43] and addition of sample buffer with or without β-mercaptoethanol. Forty micrograms of total protein were loaded on a 15% SDS-PAGE gel, followed by anti-HA Western Blot (Sigma–Aldrich, 1:2000) to visualize the monomeric form of Trx-1. This experiment was performed once.

To study if ADAM17 full-length can influence the oligomer state of endogenous Trx-1, extract from cells overexpressing ADAM17-HA (Flp-In HA-ADAM17) or knockdown for ADAM17 gene (A431/shADAM17) were analyzed on an SDS-PAGE gel. 40 μg of total cell extract (lysis buffer: 50 mM Tris-HCl pH 7.4, 150 mM NaCl, 1 mM EDTA, 1% Triton and protease inhibitor cocktail) was loaded on a 15% SDS-PAGE gel, followed by Western Blot *anti*-Trx-1 (1:2000) and anti-HA (1:2000) to visualize the monomeric form of Trx-1 and recombinant expression of ADAM17, respectively. Western Blot anti-actin (1:2000) was used for loading control. This experiment was performed once.

4.13. iodoTMT labeling

The iodoTMT experiment was performed first co-transfecting HEK293 cells with Trx-1 plus $ADAM17cyto^{WT}$ (Trx-1/$ADAM17cyto^{WT}$) or Trx-1 plus $ADAM17cyto^{F730A}$ (Trx-1/$ADAM17cyto^{F730A}$). The cells were lysed with modified RIPA buffer (25 mM HEPES, pH 8.5 containing 150 mM NaCl, 1 mM EDTA, and 1% Triton X-100) supplemented with complete protease inhibitor cocktail (Roche, Basileia, CH). Afterwards, protein quantification was performed by BCA method and 500 μg of the lysate was mixed to 0.2 mg of iodoTMT six-plex isobaric label reagent set (Thermo Fisher Scientific) (1-[126-Trx-1/$ADAM17cyto^{WT}$], 2-[127-Trx-1/$ADAM17cyto^{WT}$], 3-[128-Trx-1/$ADAM17cyto^{WT}$], 4-[129-Trx-1/$ADAM17cyto^{F730A}$], 5-[130-Trx-1/$ADAM17cyto^{F730A}$], 6-[131-Trx-1/$ADAM17cyto^{F730A}$] at room temperature for 1 h. The reaction was quenched by 10 mM DTT and incubated in the dark for 15 min. After, 20% trichloroacetic acid (TCA) precipitation, the protein pellet was digested with 6 μg LysC (Wako, Japan) for 2 h at 37 °C. Protein extracts were further diluted to 2 M urea, and subjected to an additional 6 μg LysC digestion overnight. Finally, protein extracts were diluted to 1.5 M urea, and 6 μg modified trypsin (Promega, Madison, WI) was added for 3 h at 37 °C. The peptides were then desalted with 50 mg Waters Sep-Pak C18 columns and eluted with 50% (v/v) acetonitrile and 0.1% (v/v) trifluoroacetic acid (TFA).

For peptide enrichment, the samples were lyophilized and re-dissolved in 600 μL of TBS buffer (25 mM Tris-HCl, pH 7.5, 0.15 M NaCl). 100 μL of settled immobilized *anti*-TMT antibody resin was

employed for the enrichment of every 1 mg labeled sample at 4 °C. After the supernatant was removed, the resin was washed three times with one column volume of TBS and three times with one column volume of deionized water. Peptides were finally eluted with four column volumes of elution buffer [10 mM *cis*-2,6-dimethylpiperidine (2,6-DMPp)/50/500 mM tetraethylammonium bicarbonate (TEAB), pH 8.5 [55], dried on vacuum concentrator, resuspended in 25% acetonitrile/0.1% formic acid and injected directly (~2 μg/μL) onto the Orbitrap Fusion mass spectrometer. Three independent experiments were performed.

4.14. LC-MS/MS for iodoTMT labeled proteins

All spectra were acquired using an Orbitrap Fusion mass spectrometer (Thermo Scientific, Watlham, MA) in line with an Easy-nLC 1000 (Thermo Fisher Scientific, Watlham, MA) ultra-high pressure liquid chromatography pump. Peptides (~1 μg) were separated in a column packed in-house with a 100 μm inner diameter containing 1 cm of Magic C4 resin (5 μm, 100 Å, Michrom Bioresources, Auburn, CA) followed by ~30 cm of GP-18 resin (1.8 μm, 200 Å; Sepax, Newark, DE) with a gradient consisting of 9–30% acetonitrile containing 0.125% formic acid over 180 min at ~250 nL/min. For all LC-MS/MS experiments, the mass spectrometer was operated in the data-dependent mode.

For the Synchronous-Precursor-Selection (SPS-MS^3) analysis with the Orbitrap Fusion Classic mass spectrometer (Thermo Scientific, Watlham, MA) the scan sequence began with an MS^1 spectrum (resolution 120,000; mass range 400–1400 *m/z*; AGC target 5×10^5; maximum injection time 250 ms). Precursors for MS^2/MS^3 analysis were selected using a Top10 method. MS^2 analysis consisted of collision-induced dissociation (CID); AGC 1.8×10^4; normalized collision energy (NCE) of 35%; maximum injection time of 120 ms; and isolation window of 0.7 Da. Following the acquisition of each MS^2 spectrum, we collected an MS^3 spectrum using the recently described method in which multiple MS^2 fragment ions (10 MS^2 fragment ions) were captured in the MS^3 precursor population using isolation waveforms with multiple frequency notches (multi-notch MS^3) (McAlister et al., 2014). MS^3 precursors were fragmented by higher-energy collisional dissociation (HCD) and analyzed in the Orbitrap (NCE 55%; AGC 1.0×10^5; maximum injection time of 120 ms, resolution was 60,000 at 400 Th).

4.15. Data processing for iodoTMT analysis

Searches were performed with Sequest using a 50 ppm precursor ion tolerance and 1Da for fragment [56]. Only peptide sequences with both termini consistent with the protease specificity of trypsin were considered in the database search, and up to two missed cleavages were accepted. IodoTMT tags on cysteine residues (+329.22659 Da) was set as static modifications, while methionine oxidation (+15.99492 Da) was set as a variable modification.

An MS^2 spectral assignment false discovery rate of less than 1% was achieved by applying the target-decoy strategy [57]. Filtering was performed using an in-house linear discrimination analysis algorithm described previously [58] to create one composite score from the following peptide ion and MS^2 spectra properties: XCorr, ΔCn score, peptide ion mass accuracy, peptide length and missed-cleavages. The resulting discriminant scores were used to sort peptides prior to filtering to a 1% FDR. Following spectral assignment, peptides were assembled into proteins and further filtered based on the combined probabilities of their constituent peptides to a final FDR of 1%. In cases of redundancy, shared peptides were assigned to the protein sequence with the most matching peptides, thus adhering to principles of parsimony [59].

4.16. Quantitative data analysis and data presentation

A compilation of in-house software was used to convert the Thermo RAW files to mzXML format, as well as to adjust monoisotopic *m/z* measurements and erroneous peptide charge state assignments. Using Sequest, MS^2 spectra were searched against the Human UniProt database (April 2nd, 2014, 71,882 total sequences), including sequences of common contaminating proteins. This database was followed forward by a decoy component. To evaluate the proteins that were significantly different in the presence of ADAM17cyto^{WT} and ADAM17cyto^{F730A}, we used the two-tailed *t*-test with unequal variance. A false discovery rate (FDR) of 1% was considered using the Benjamin-Hochberg method with the in-house development tool. All the 821 proteins that were quantified in the multi-notch MS^3 data, considering single (only one) and composite (two or more) cysteine sites in the iodoTMT experiment, were analyzed and presented in the Supplementary Table 7-8.

4.17. Bioinformatic analysis

GO annotation of molecular function for the differential proteins was performed using BinGO plugin 3.0.3 with Cytoscape 3.7.1, with the significance threshold set at P-value <0.05 using the Hypergeometric test. The whole human proteome Gene Ontology (GO) annotation file was used as reference set. Overrepresented GO terms are represented as bar plots according to the P-value of the enrichment analysis (Supplementary Table 9). The fold enrichment was calculated between the enriched terms for the upregulated proteins and the downregulated proteins (Supplementary Table 10).

4.18. Statistical analysis

For the statistical analysis of solid-phase binding assay, Trx-1 reductive activity, ADAM17 activity by AP reporter activity, measurement of H_2O_2 production, and reactivity of cysteines by AmplexRed and DTNB, we performed Student's *t*-test or one-way ANOVA followed by Tukey's or Bonferroni's posttest. The significance level was stated at $p < 0.05$ (GraphPad Prism version 5 for Windows, California, U.S.A).

5. Data availability

The mass spectrometry proteomics data have been deposited in the ProteomeXchange Consortium (http://proteomecentral.proteomexchange.org) via the PRIDE partner repository [60] with the dataset identifier PXD015431 (https://www.ebi.ac.uk/pride/archive/projects/PXD015431). The SRM analyses for the seven measured proteins are available through the Panorama repository at the following link (https://panoramaweb.org/7j9Lbk.url). Skyline exported data for all quantified peptides are available in Supplementary Tables 4 and 6 All other data supporting the findings of this study are available from the corresponding author on request.

Funding and additional information

Funding was provided by FAPESP Grants (2009/54067–3; 2010/19278–0, 2016/07846–0,2014/23888–0, 2018/18496-6 to AFPL; 2014/06485–9 and 2016/01528–7 to RAPC; 2018/15535–0 to DCG; 2018/12194–8 to LDT; 2016/24664–3 to AGS; 305748/2017-3> and 428527/2018-3 to FMS) and CNPq Grants (470549/2011–4 and 305851/2017–9 to AFPL; 150221/2014–2 to DCG).

Declaration of competing interest

The authors had no conflicts of interest concerning the topic under consideration in this article.

Acknowledgements

We appreciated the suggestions in enzyme kinetics from Dr. André Damásio and Carolline Ascensão. We would like to thank Waters Corporation for providing us with access to Xevo TQ-XS triple quadrupole mass spectrometer. We acknowledge the Mass Spectrometry Laboratory,

Spectroscopy and Colorimetry Laboratory, and Laboratory of Protein purification at Brazilian Biosciences National Laboratory, CNPEM, Campinas, Brazil for their support with the analyses.

Appendix A. Supplementary data

Supplementary data to this article can be found online at https://doi.org/10.1016/j.redox.2020.101735.

References

[1] E. Arnér, A. Holmgren, Measurement of thioredoxin and thioredoxin reductase (Chapter 7), Curr. Protoc. Toxicol. 24 (1) (2001) 7.4.1–7.4.14, https://doi.org/10.1002/0471140856.tx0704s05. Unit 7.4.

[2] M. Gooz, ADAM-17: the enzyme that does it all, Crit. Rev. Biochem. Mol. Biol. 45 (2010) 146–169, https://doi.org/10.3109/10409231003628015.

[3] K.A. Papadakis, S.R. Targan, Role of cytokines in the pathogenesis of inflammatory bowel disease, Annu. Rev. Med. 51 (2000) 289–298, https://doi.org/10.1146/annurev.med.51.1.289.

[4] M. Feldmann, F.M. Brennan, R.N. Maini, Role OF cytokines IN rheumatoid arthritis, Annu. Rev. Immunol. 14 (1996) 397–440, https://doi.org/10.1146/annurev.immunol.14.1.397.

[5] D.N. Meli, J.M. Loeffler, P. Baumann, U. Neumann, T. Buhl, D. Leppert, S.L. Leib, In pneumococcal meningitis a novel water-soluble inhibitor of matrix metalloproteinases and TNF-α converting enzyme attenuates seizures and injury of the cerebral cortex, J. Neuroimmunol. 151 (2004) 6–11, https://doi.org/10.1016/j.jneuroim.2004.01.026.

[6] M. Katakowski, F. Jiang, X.G. Zheng, J.A. Gutierrez, A. Szalad, M. Chopp, Tumorigenicity of cortical astrocyte cell line induced by the protease ADAM17, Canc. Sci. 100 (2009) 1597–1604, https://doi.org/10.1111/j.1349-7006.2009.01221.x.

[7] A. Mahmud-Al-Rafat, A. Majumder, K.M. Taufiqur Rahman, A.M. Mahedi Hasan, K. M. Didarul Islam, A.W. Taylor-Robinson, M.M. Billah, Decoding the enigma of antiviral crisis: does one target molecule regulate all? Cytokine 115 (2019) 13–23, https://doi.org/10.1016/j.cyto.2018.12.008.

[8] D. Ragab, H. Salah Eldin, M. Taeimah, R. Khattab, R. Salem, The COVID-19 cytokine storm; what we know so far, Front. Immunol. 11 (2020) 1446. https://www.frontiersin.org/article/10.3389/fimmu.2020.01446.

[9] D.C. Blaydon, P. Biancheri, W.-L. Di, V. Plagnol, R.M. Cabral, M.A. Brooke, D. A. van Heel, F. Ruschendorf, M. Toynbee, A. Walne, E.A. O'Toole, J.E. Martin, K. Lindley, T. Vulliamy, D.J. Abrams, T.T. MacDonald, J.I. Harper, D.P. Kelsell, Inflammatory skin and bowel disease linked to ADAM17 deletion, N. Engl. J. Med. 365 (2011) 1502–1508, https://doi.org/10.1056/NEJMoa1100721.

[10] J. Arribas, C. Esselens, ADAM17 as a therapeutic target in multiple diseases, Curr. Pharmaceut. Des. 15 (2009) 2319–2335, https://doi.org/10.2174/138161209788682398.

[11] J. Scheller, A. Chalaris, C. Garbers, S. Rose-John, ADAM17: a molecular switch to control inflammation and tissue regeneration, Trends Immunol. 32 (2011) 380–387, https://doi.org/10.1016/j.it.2011.05.005.

[12] D.W. Lambert, M. Yarski, F.J. Warner, P. Thornhill, E.T. Parkin, A.I. Smith, N. M. Hooper, A.J. Turner, Tumor necrosis factor-α convertase (ADAM17) mediates regulated ectodomain shedding of the severe-acute respiratory syndrome-coronavirus (SARS-CoV) receptor, angiotensin-converting enzyme-2 (ACE2), J. Biol. Chem. 280 (2005) 30113–30119, https://doi.org/10.1074/jbc.M505111200.

[13] S. Haga, N. Yamamoto, C. Nakai-Murakami, Y. Osawa, K. Tokunaga, T. Sata, N. Yamamoto, T. Sasazuki, Y. Ishizaka, Modulation of TNF-α-converting enzyme by the spike protein of SARS-CoV and ACE2 induces TNF-α production and facilitates viral entry, Proc. Natl. Acad. Sci. U. S. A. 105 (2008) 7809–7814, https://doi.org/10.1073/pnas.0711241105.

[14] Q. Ye, B. Wang, J. Mao, The pathogenesis and treatment of the 'Cytokine Storm' in COVID-19, J. Infect. 80 (2020) 607–613, https://doi.org/10.1016/j.jinf.2020.03.037.

[15] Y.-M. Gao, G. Xu, B. Wang, B.-C. Liu, Cytokine storm syndrome in coronavirus disease 2019: a narrative review, J. Intern. Med. (2020), https://doi.org/10.1111/joim.13144.

[16] P. Rizzo, F. Vieceli Dalla Sega, F. Fortini, L. Marracino, C. Rapezzi, R. Ferrari, COVID-19 in the heart and the lungs: could we "Notch" the inflammatory storm? Basic Res. Cardiol. 115 (2020) 1–8, https://doi.org/10.1007/s00395-020-0791-5.

[17] K. El Hadri, M. Dler Faieeq Darweesh, D. Couchie, I. Jguirim-Souissi, F. Genze, V. Diderot, T. Syrovets, O. Lunov, T. Simmet, M. Rouis, Thioredoxin-1 promotes anti-inflammatory macrophages of the M2 phenotype and antagonizes atherosclerosis, Arterioscler. Thromb. Vasc. Biol. 32 (2012) 1445–1452, https://doi.org/10.1161/ATVBAHA.112.249334.

[18] H. Sies, D.P. Jones, Reactive oxygen species (ROS) as pleiotropic physiological signalling agents, Nat. Rev. Mol. Cell Biol. 21 (2020) 363–383, https://doi.org/10.1038/s41580-020-0230-3.

[19] J. Muri, H. Thut, Q. Feng, M. Kopf, Thioredoxin-1 distinctly promotes NF-kB target dna binding and nlrp3 inflammasome activation independently of txnip, Elife 9 (2020) 1–30, https://doi.org/10.7554/eLife.53627.

[20] R. Watanabe, H. Nakamura, H. Masutani, J. Yodoi, Anti-oxidative, anti-cancer and anti-inflammatory actions by thioredoxin 1 and thioredoxin-binding protein-2, Pharmacol. Ther. 127 (2010) 261–270, https://doi.org/10.1016/j.pharmthera.2010.04.004.

[21] R. Zhou, A. Tardivel, B. Thorens, I. Choi, J. Tschopp, Thioredoxin-interacting protein links oxidative stress to inflammasome activation, Nat. Immunol. 11 (2010) 136–140, https://doi.org/10.1038/ni.1831.

[22] S. Salzano, P. Checconi, E.-M. Hanschmann, C.H. Lillig, L.D. Bowler, P. Chan, D. Vaudry, M. Mengozzi, L. Coppo, S. Sacre, K.R. Atkuri, B. Sahaf, L.A. Herzenberg, L.A. Herzenberg, L. Mullen, P. Ghezzi, Linkage of inflammation and oxidative stress via release of glutathionylated peroxiredoxin-2, which acts as a danger signal, Proc. Natl. Acad. Sci. U. S. A. 111 (2014) 12157–12162, https://doi.org/10.1073/pnas.1401712111.

[23] Y.M. Go, P.J. Halvey, J.M. Hansen, M. Reed, J. Pohl, D.P. Jones, Reactive aldehyde modification of thioredoxin-1 activates early steps of inflammation and cell adhesion, Am. J. Pathol. 171 (2007) 1670–1681, https://doi.org/10.2353/ajpath.2007.070218.

[24] A. Weichsel, J.R. Gasdaska, G. Powis, W.R. Montfort, Crystal structures of reduced, oxidized, and mutated human thioredoxins: evidence for a regulatory homodimer, Structure 4 (1996) 735–751, https://doi.org/10.1016/S0969-2126(96)00079-2.

[25] K.T. Barglow, C.G. Knutson, J.S. Wishnok, S.R. Tannenbaum, M.A. Marletta, Site-specific and redox-controlled S-nitrosation of thioredoxin, Proc. Natl. Acad. Sci. U. S. A. 108 (2011), https://doi.org/10.1073/pnas.1110736108.

[26] Y. Du, H. Zhang, X. Zhang, J. Lu, A. Holmgren, Thioredoxin 1 is inactivated due to oxidation induced by peroxiredoxin under oxidative stress and reactivated by the glutaredoxin system, J. Biol. Chem. 288 (2013) 32241–32247, https://doi.org/10.1074/jbc.M113.495150.

[27] A.Z.B. Aragão, M.L.C. Nogueira, D.C. Granato, F.M. Simabuco, R.V. Honorato, Z. Hoffman, S. Yokoo, F.R.M. Laurindo, F.M. Squina, A.C.M. Zeri, P.S.L. Oliveira, N.E. Sherman, A.F. Paes Leme, Identification of novel interaction between ADAM17 (a disintegrin and metalloprotease 17) and thioredoxin-1, J. Biol. Chem. 287 (2012) 43071–43082, https://doi.org/10.1074/jbc.M112.364513.

[28] D.C. Granato, R.A.P. e Costa, R. Kawahara, S. Yokoo, A.Z. Aragão, R.R. Domingues, B.A. Pauletti, R. V Honorato, J. Fattori, A.C.M. Figueira, P.S.L. Oliveira, S. R. Consonni, D. Fernandes, F. Laurindo, H.P. Hansen, A.F. Paes Leme, Thioredoxin-1 negatively modulates ADAM17 activity through direct binding and indirect reductive activity, Antioxidants Redox Signal. 29 (2018) 717–734, https://doi.org/10.1089/ars.2017.7297.

[29] A. Holmgren, Thioh.edoxin 54 (1985) 237–271.

[30] S.K. Katti, D.M. LeMaster, H. Eklund, Crystal structure of thioredoxin from Escherichia coli at 1.68 A resolution, J. Mol. Biol. 212 (1990) 167–184, https://doi.org/10.1016/0022-2836(90)90313-B.

[31] X. Ren, M. Bjoernstedt, B. Shen, M.L. Ericson, A. Holmgren, Mutagenesis of structural half-cystine residues in human thioredoxin and effects on the regulation of activity by selenodiglutathione, Biochemistry 32 (1993) 9701–9708, https://doi.org/10.1021/bi00088a023.

[32] A. Holmgren, System 252 (1977) 4600–4606.

[33] Y. Zhang, J. Park, S.J. Han, S.Y. Yang, H.J. Yoon, I. Park, H.A. Woo, S.R. Lee, Redox regulation of tumor suppressor PTEN in cell signaling, Redox Biol 34 (2020) 101553, https://doi.org/10.1016/j.redox.2020.101553.

[34] A.A. Campos-Acevedo, R.R. Sotelo-Mundo, J. Pérez, E. Rudiño-Piñera, Is dimerization a common feature in thioredoxins? The case of thioredoxin from {\it Litopenaeus vannamei}, Acta Crystallogr. D 73 (2017) 326–339, https://doi.org/10.1107/S2059798317002066.

[35] M. Qin, W. Wang, D. Thirumalai, Protein folding guides disulfide bond formation, Proc. Natl. Acad. Sci. U. S. A. 112 (2015) 11241–11246, https://doi.org/10.1073/pnas.1503909112.

[36] Y. Taniyama, R. Kuroki, F. Omura, C. Seko, M. Kikuchi, Evidence for intramolecular disulfide bond shuffling in the folding of mutant human lysozyme, J. Biol. Chem. 266 (1991) 6456–6461.

[37] G. Roos, N. Foloppe, K. Van Laer, L. Wyns, L. Nilsson, P. Geerlings, J. Messens, How thioredoxin dissociates its mixed disulfide, PLoS Comput. Biol. 5 (2009), e1000461, https://doi.org/10.1371/journal.pcbi.1000461.

[38] K. Kolšek, C. Aponte-Santamaría, F. Gräter, Accessibility explains preferred thiol-disulfide isomerization in a protein domain, Sci. Rep. 7 (2017) 9858, https://doi.org/10.1038/s41598-017-07501-4.

[39] S.H. Willems, C.J. Tape, P.L. Stanley, N.A. Taylor, I.G. Mills, D.E. Neal, J. McCafferty, G. Murphy, Thiol isomerases negatively regulate the cellular shedding activity of ADAM17, Biochem. J. 428 (2010) 439–450, https://doi.org/10.1042/BJ20100179.

[40] A. Brill, A. Chauhan, M. Canault, M. Walsh, W. Bergmeier, D. Wagner, Oxidative stress activates ADAM17/TACE and induces its target receptor shedding in platelets in a p38-dependent fashion, Cardiovasc. Res. 84 (2009) 137–144, https://doi.org/10.1093/cvr/cvp176.

[41] W. Jeong, T.S. Chang, E.S. Boja, H.M. Fales, S.G. Rhee, Roles of TRP14, a thioredoxin-related protein in tumor necrosis factor-α signaling pathways, J. Biol. Chem. 279 (2004) 3151–3159, https://doi.org/10.1074/jbc.M307959200.

[42] W. Jeong, Y. Jung, H. Kim, S.J. Park, S.G. Rhee, Thioredoxin-related protein 14, a new member of the thioredoxin family with disulfide reductase activity: implication in the redox regulation of TNF-alpha signaling, Free Radic. Biol. Med. 47 (2009) 1294–1303, https://doi.org/10.1016/j.freeradbiomed.2009.07.021.

[43] P.J. Nadeau, S.J. Charette, M.B. Toledano, J. Landry, Disulfide Bond-mediated multimerization of Ask1 and its reduction by thioredoxin-1 regulate H(2)O(2)-induced c-Jun NH(2)-terminal kinase activation and apoptosis, Mol. Biol. Cell 18 (2007) 3903–3913, https://doi.org/10.1091/mbc.e07-05-0491.

[44] C. Hegedűs, K. Kovács, Z. Polgár, Z. Regdon, É. Szabó, A. Robaszkiewicz, H. J. Forman, A. Martner, L. Virág, Redox control of cancer cell destruction, Redox Biol 16 (2018) 59–74, https://doi.org/10.1016/j.redox.2018.01.015.

[45] S. Düsterhöft, K. Höbel, M. Oldefest, J. Lokau, G.H. Waetzig, A. Chalaris, C. Garbers, J. Scheller, S. Rose-John, I. Lorenzen, J. Grötzinger, A disintegrin and metalloprotease 17 dynamic interaction sequence, the sweet tooth for the human interleukin 6 receptor, J. Biol. Chem. 289 (2014) 16336–16348, https://doi.org/10.1074/jbc.M114.557322.
[46] S. Düsterhöft, S. Jung, C.-W. Hung, A. Tholey, F.D. Sönnichsen, J. Grötzinger, I. Lorenzen, Membrane-proximal domain of a disintegrin and metalloprotease-17 represents the putative molecular switch of its shedding activity operated by protein-disulfide isomerase, J. Am. Chem. Soc. 135 (2013) 5776–5781, https://doi.org/10.1021/ja400340u.
[47] P. Chakraborty, S. Chatterjee, P. Kesarwani, K. Thyagarajan, S. Iamsawat, A. Dalheim, H. Nguyen, S.P. Selvam, P. Nasarre, G. Scurti, G. Hardiman, N. Maulik, L. Ball, V. Gangaraju, M.P. Rubinstein, N. Klauber-DeMore, E.G. Hill, B. Ogretmen, X.Z. Yu, M.I. Nishimura, S. Mehrotra, Thioredoxin-1 improves the immunometabolic phenotype of antitumor T cells, J. Biol. Chem. 294 (2019) 9198–9212, https://doi.org/10.1074/jbc.RA118.006753.
[48] A. Oliveira, A. Leme, A. Asega, A. Camargo, J. Fox, S. Serrano, New insights into the structural elements involved in the skin haemorrhage induced by snake venom metalloproteinases, Thromb. Haemostasis 104 (2010) 485–497, https://doi.org/10.1160/TH09-12-0855.
[49] J. Fattori, J.L.O. Campos, T.R. Doratioto, L.M. Assis, M.T. Vitorino, I. Polikarpov, J. Xavier-Neto, A.C.M. Figueira, RXR agonist modulates TR: corepressor dissociation upon 9-cis retinoic acid treatment, Mol. Endocrinol. 29 (2015) 258–273, https://doi.org/10.1210/me.2014-1251.
[50] C. Tu, Q. Sheng, J. Li, D. Ma, X. Shen, X. Wang, Y. Shyr, Z. Yi, J. Qu, Optimization of search engines and postprocessing approaches to maximize peptide and protein identification for high-resolution mass data, J. Proteome Res. 14 (2015) 4662–4673, https://doi.org/10.1021/acs.jproteome.5b00536.
[51] K.M. Pearson, L.K. Pannell, H.M. Fales, Intramolecular cross-linking experiments on cytochrome c and ribonuclease A using an isotope multiplet method, Rapid Commun. Mass Spectrom. 16 (2002) 149–159, https://doi.org/10.1002/rcm.554.
[52] B. Schilling, R.H. Row, B.W. Gibson, X. Guo, M.M. Young, MS2Assign, automated assignment and nomenclature of tandem mass spectra of chemically crosslinked peptides, J. Am. Soc. Mass Spectrom. 14 (2003) 834–850, https://doi.org/10.1016/S1044-0305(03)00327-1.
[53] P. Schuck, Size-distribution analysis of macromolecules by sedimentation velocity ultracentrifugation and Lamm equation modeling, Biophys. J. 78 (2000) 1606–1619, https://doi.org/10.1016/S0006-3495(00)76713-0.
[54] S.M. Le Gall, T. Maretzky, P.D.A. Issuree, X. Da Niu, K. Reiss, P. Saftig, R. Khokha, D. Lundell, C.P. Blobel, ADAM17 is regulated by a rapid and reversible mechanism that controls access to its catalytic site, J. Cell Sci. 123 (2010) 3913–3922, https://doi.org/10.1242/jcs.069997.
[55] Z. Qu, F. Meng, R.D. Bomgarden, R.I. Viner, J. Li, J.C. Rogers, J. Cheng, C. M. Greenlief, J. Cui, D.B. Lubahn, G.Y. Sun, Z. Gu, Proteomic quantification and site-mapping of S -nitrosylated proteins using isobaric iodoTMT reagents, J. Proteome Res. 13 (2014) 3200–3211, https://doi.org/10.1021/pr401179v.
[56] S.A. Beausoleil, J. Villen, S.A. Gerber, J. Rush, S.P. Gygi, A probability-based approach for high-throughput protein phosphorylation analysis and site localization, Nat. Biotechnol. 24 (2006) 1285–1292, https://doi.org/10.1038/nbt1240.
[57] J.E. Elias, S.P. Gygi, Target-decoy search strategy for increased confidence in large-scale protein identifications by mass spectrometry, Nat. Methods 4 (2007) 207–214, https://doi.org/10.1038/nmeth1019.
[58] E.L. Huttlin, M.P. Jedrychowski, J.E. Elias, T. Goswami, R. Rad, S.A. Beausoleil, J. Villén, W. Haas, M.E. Sowa, S.P. Gygi, NIH Public Access 143 (2011) 1174–1189, https://doi.org/10.1016/j.cell.2010.12.001.A.
[59] V. Chvátal, M. Goldsmith, N. Yang, McCulloch-pitts brains and pseudorandom functions, Neural Comput. 28 (2016) 1042–1050, https://doi.org/10.1162/NECO_a_00841.
[60] J.A. Vizcaíno, E.W. Deutsch, R. Wang, A. Csordas, F. Reisinger, D. Ríos, J. A. Dianes, Z. Sun, T. Farrah, N. Bandeira, P.-A. Binz, I. Xenarios, M. Eisenacher, G. Mayer, L. Gatto, A. Campos, R.J. Chalkley, H.-J. Kraus, J.P. Albar, S. Martinez-Bartolomé, R. Apweiler, G.S. Omenn, L. Martens, A.R. Jones, H. Hermjakob, ProteomeXchange provides globally coordinated proteomics data submission and dissemination, Nat. Biotechnol. 32 (2014) 223–226, https://doi.org/10.1038/nbt.2839.

ABBREVIATIONS AND NOMENCLATURE

ANOVA: analysis of variance
FDR: false discovery rate
GO: gene ontology
HB-EGF-AP: heparin-binding epidermal growth factor in fusion with alkaline phosphatase
iodoTMT: iodo-Tandem Mass Tags
MS: mass spectrometry
PMA: phorbol 12-myristate 13-acetate
ROS: reactive oxygen species
Trx-1: thioredoxin-1
TrxR1: thioredoxin reductase 1